Sliding Mode Control Applied To UPS Inverter Using Norm of the State Error

Hamza A. M. Makhamreh

Submitted to the
Institute of Graduate Studies and Research
in partial fulfillment of the requirements for the Degree of

Master of Science
in
Electrical and Electronic Engineering

Eastern Mediterranean University
February 2013
Gazimağusa, North Cyprus

Approval of the Institute of Graduate Studies and Research

Prof. Dr. Elvan Yılmaz
Director

I certify that this thesis satisfies the requirements as a thesis for the degree of Master of Science in Electrical and Electronic Engineering.

Prof. Dr. Aykut Hocanın
Chair, Department of Electrical Electronic and Engineering

We certify that we have read this thesis and that in our opinion it is fully adequate in scope and quality as a thesis for the degree of Master of Science in Electrical and Electronic Engineering.

Prof. Dr. Osman Kukrer
Supervisor

Examining Committee

1. Prof. Dr. Hasan Kömürcügil
2. Prof. Dr. Osman Kukrer
3. Prof. Dr. Runyi Yu

ABSTRACT

In dynamical system it is impossible to avoid dealing with uncertain conditions such as disturbances; that case is applicable on the UPS Inverter. There are many approaches to control inverters; here we are going to introduce a new approach of sliding mode control applied to UPS inverters.

We reduce the sliding time of the state trajectory, by defining a function with respect to the error norm. This function gives the system a value of the sliding line at each instance, such that the performance is improved. The function is defined as the norm of both voltage error and its derivative multiplied by a factor. The norm value is saturated for small and large value of λ, which represents the slope of the sliding line. Another parameter (β) is also introduced, which is a gain multiplying the result of the saturated function.

When the state is far from the origin, small value of λ is used in the reaching mode, while large value of λ is used when the state reaches the sliding line and start to "slide" on the sliding line. From the definition of the norm error, a function is derived which is used to minimize the reaching time. The results of simulation are compared to Three level hysteresis and rotating sliding mode approaches. The new approach shows a fast response with very small value of the voltage error.

Keywords: uninterruptible power supply, inverters, sliding mode control, rotating sliding line.

ÖZ

Dinamik sistemlerde bozan etkenler gibi belirsiz durumlarla karşılaşmak mümkündür. Bu çevirgeçler için de geçerlidir. Çevirgeçleri kontrol etmek için bir çok yaklaşım vardır. Bu çalışmada Kesintisiz Güç Kaynak (KGK) çevirgeçlerin kontrolu için yeni bir kayan kipli kontrol yöntemi önerilmektedir.

Hata dizgesine bağlı bir işlev tanımlamak suretiyle durum gezingesinin kayma zamanını kısaltmak mümkündür. Bu işlev kayma çizgisine her an yeni bir eğim vererek başarımı artırmaktadır. Bu işlev çıkış voltajı ve türevinin düzgesi olarak tanınlanmaktadır. Düzge değeri kayma çizgisinin eğiminin çok küçük ve çok büyük değerleri için doyuma ulaşır. Bu doyumlu işlevi çarpan bir parametre (β) daha tanımlanmıştır.

Durum vektörü merkezden uzak olduğunda ve erişme kipi sırasında λ için küçük, durum vektörü kayma çizgisine ulaştığında ve bunun üzerinde kaymaya başladığında ise büyük bir değer kullanılır. Düzgenin tanımından hareketle kayma zamanını en aza indigemede kullanılabilecek bir işlev elde edilmiştir. Benzetim sonuçları üç-seviyeli histerisis ve dönen kayma kipli yöntemleri ile karşılaştırılmıştır. Önerilen yöntemin daha hızlı tepki ve daha düşük voltaj hatası verdiği gözlenmiştir.

Anahtar kelimeler: Kesintisiz Güç Kaynakları, Çevirgeçler, Kayan Kipli Kontrol, Dönen Kayma Çizgisi.

To:

My Beloved Uncle, Abu Nedal.

ACKNOWLEDGMENTS

It would not have been possible to write this thesis without the help and support of the kind people around me, to only some of whom it is possible to give particular mention here.

Especially, I would like to thank my supervisor Prof. Osman Kukrer for his patience, support and immense knowledge in all aspect of my research. He teaches me how to understand, think, analyze then conclude the results.

I would like to thank the chairman of Electrical and Electronic department Prof. Aykut Hocanin for his good advice, support and friendship dealing with us. His support has been invaluable on both an academic and a personal level, for which I am extremely grateful.

My parents, brother and sister have given me their obvious support throughout, as always, for which my simple expression of thanks likewise does not suffice. Special Thanks goes to my favorite uncle “Abu Nedal” and his Great wife “Kamela” for their care, interest, and support in all phases of my life.

I am most grateful to my best friend Derar Zedan and Ahmed Yassin for supporting me each moment I spend in Cyprus.

I do not forget that, the first and last thanks is all for our God.

TABLE OF CONTENTS

LIST OF TABLES

LIST OF FIGURES

LIST OF ABBREVIATIONS

CSI	Current Source Inverter
DOF	Degree Of Freedom
EMI	Electromagnetic Interface
ERL	Exponential Reaching Law
FPGA	Field Programmable Gate Array
GTO	Gate Turn-off Thyristor
IGBT	Insulated-Gate Bipolar Transistor
ILC	Iterative Learning Control
IMP	Internal Model Principle
LCI	Load Commutated Inverter
MOSFET	Metal Oxide Semiconductor Field Effect Transistor
MRAC	Model Reference Adaptive Control
PID	Proportional- Integral Derivative Controller
PWM	Pulse Width Modulation
STC	Self Tuning Controller
VSC	Variable Structure Control
VSI	Voltage Source Inverter

Chapter1

INTRODUCTION

1.1 Inverters

An inverter is a power electronic device which transfers one or multiple DC voltage or current sources to an adjustable switching pattern (AC waveform). The output will be amplitude-, frequency- and phase shift-controllable through control signals to the switched power devices. Figure 1.1 shows the general construction of a DC/AC power converter (inverter), with a fixed input DC current/voltage and variable AC output waveform.

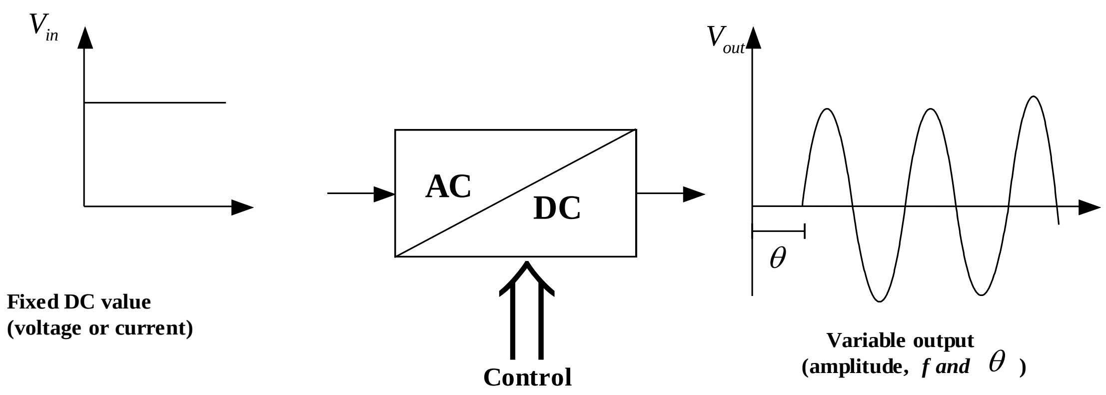

Figure 1.1: General configuration of DC/AC converter [1].

It's possible to classify the types of inverters depending on the input type. Generally we have voltage source inverters (VSI), with DC input voltage, and current source inverters (CSI) with DC current source. The DC voltage could be configured by a rectifier followed by a capacitor; such conversion is called *indirect* *conversion* (AC-DC/DC-AC conversion). It's also possible to have a DC source at the input of the inverter by using a DC battery, photovoltaic modules or fuel cells. It's the same for CSI; the DC current can be configured by a rectifier followed by an inductor for indirect conversion, or using traditional DC sources.

As mentioned before, the inverters are classified as CSI and VSI, and we can classify them depending on the amount of output power. It's noticeable that the CSI are used in medium and high power conversion by using Pulse Width Modulation (PWM-CSI), or the Load Commutated Inverter (LCI). VSI's are used for the application of medium and high power systems, by using a two-level approach for single-phase and three-phase inverters in low/medium power applications, and multilevel approach for medium/high power applications. Here we are going to discuss single-phase half bridge and full bridge VSI, in sections 1.2 and 1.3 respectively. The application will follow in section 1.4.

1.2 Single-Phase Half Bridge Inverter

Figure 1.2.a shows the general configuration of a single-phase half bridge inverter, consisting of one leg of semiconductor switches Q1 and Q2, each of them having a diode in parallel. The diodes D1 and D2 allow for the negative current to flow in the opposite direction. Q1 and D1 together are called a *Bidirectional Switch* and the same is true for Q2 and D2.

Two series capacitors are connected in parallel with the Dc source. These capacitors divide the source into two equivalent values (if C1=C2), and provide a neutral point (0) between them for the load to be connected to. The switches Q1and Q2 could be any power switch like GTO, IGBT or MOSFET.

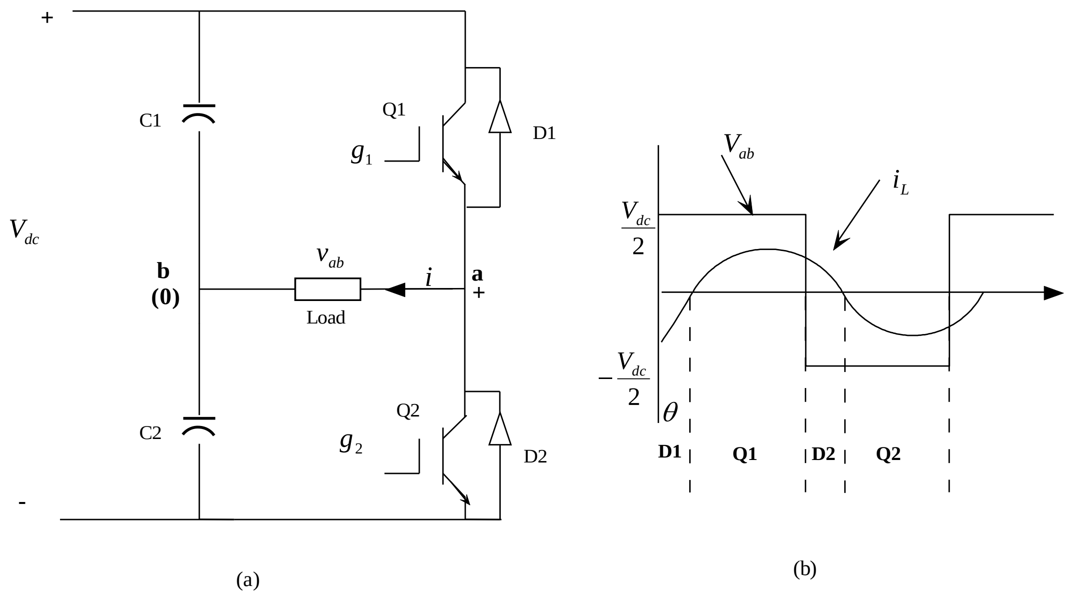

Figure 1.2: (a) Single Phase Half Bridge Inverter, and (b) output voltage and current waveforms [1].

Referring to Figure 1.2(a), notice that transistors Q1 and Q2 are controlled by control signals g1 and g2 respectively. The control signal g1 can have the values $\{0, 1\}$. When the control signal is 1, which means that the switch is ON, then the supply voltage will be connected to terminal a, and the output voltage $V_{ab} = \frac{V_{dc}}{2}$. And when the control signal is 0, then the switch will be OFF, and the output voltage $V_{ab} = -\frac{V_{dc}}{2}$. Notice that the output voltage is alternating between$\left\{\frac{V_{dc}}{2}\ and -\frac{V_{dc}}{2}\right\}$; which means that we have *two level* output voltage, as shown in Figure 1.2.b). Practically a dead time is left between turning on Q2 and turning off Q1 or the opposite, which ensures that the switches will not short circuit the source voltage.

1.3 Single Phase Full Bridge Inverter

Figure 1.3(a) shows the general construction for a single-phase full bride inverter, or H- Bridge inverter. The inverter consists of two half bridge inverters but without the capacitors on the input, each leg of the inverter has two bidirectional switches (power switch in parallel with freewheeling diode) in series, and the load is connected to the midpoint of each leg (to the points a and b). As mentioned before in the half bridge inverter, the power switch could be any power device (MOSEFET or IGBT).

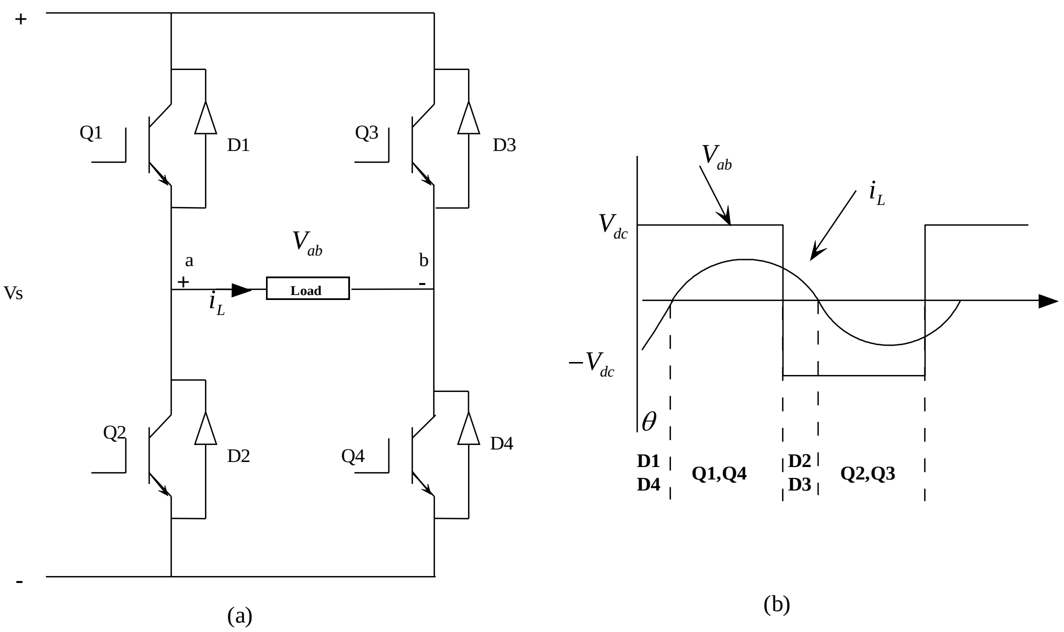

Figure 1.3: (a) Single Phase full Bridge Inverter, and (b) output voltage and current waveforms for square wave operation [2].

The control signals will be applied to the gates g1 and g4, while its logic inverse will be applied to g2 and g3. For instance, if we consider square wave operation, when we apply logic “1” on g1 and g2 (i.e. ON), then the positive load voltage will be connected to point a through Q1, and the negative supply voltage will be connected to terminal b through Q4, which means that V_{dc} V_{dc} appears on the output. Following the same logic for Q2 and Q3, we will have -V_{dc} $-V_{dc}$on the output as shown above in Figure 1.3, this figure shows also the current waveform for highly inductive load, neglecting the harmonics, and with phase shift θ (lagging) for the current.

1.4 Inverter Applications

UPS inverters are used to supply loads with the necessary AC power during power failures, for instance medical/life support systems, computers, and communication systems. The main task of the UPS system is to maintain a fixed voltage supplied to the load with a fixed frequency for vital load, whatever discrepancies arise at the load. For the application of UPS, inverters are connected to a DC power supply and used as a rectifier to charge the batteries, so when the AC source fails to supply the load, the inverter pack-up the source, and transform the DC voltage source to an alternative one (AC) by mean of switching control. When the network power supply returns back, the inverter is disconnected from supplying the load and returns back to charging the batteries, as shown in Figure 1.4.

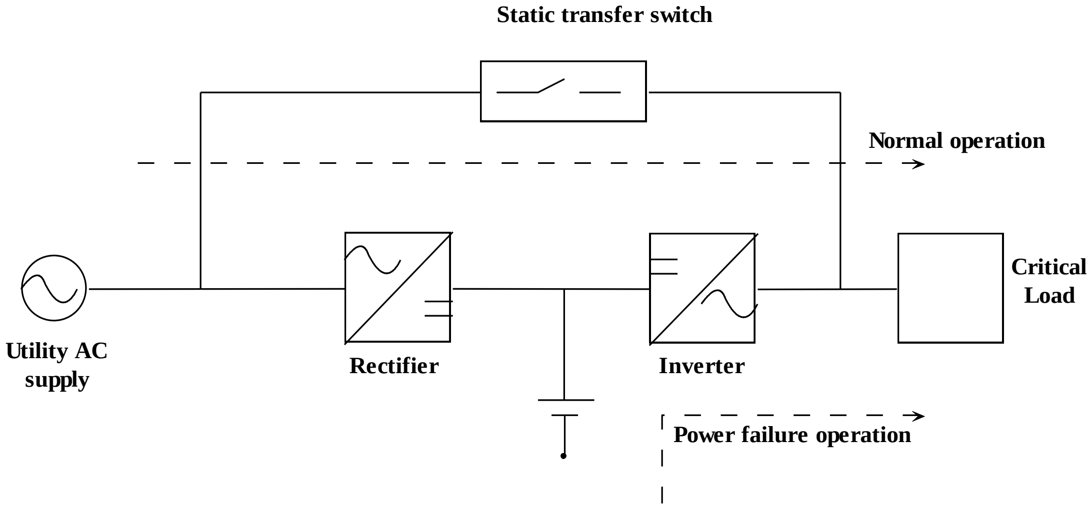

Figure 1.4: Online UPS Inverter [3].

For high performance UPS applications, the device should have pure sinusoidal output which containing low harmonic signals such that the total harmonic distortion is very low, a fast transient response for sudden load and high efficiency. The topic of this thesis is to discuss a control method which improves the above factors such that the inverter's quality is increased.

This thesis is organized as follow; firstly, we are going to represent a tutorial review for control methods used and their application to UPS inverters in chapter two. In chapter Three, the theory of Sliding mode control will be introduced; while, the new approach will be described in chapter four. Simulation and results will be presented in chapter Five, and finally with conclusion and future work in chapter six.

In this thesis we represent a new control function which is applied to a UPS inverter using sliding mode control. The aim of the function is dedicated to reduce the sliding time of the state using the norm of the error, which is produced in a combination from the voltage error x_1 and its derivative x_2. The resultant norm value in applied to saturation dynamic function which gives a high slope value when the state trajectory starts to "slide" on the sliding line. This will reduce the sliding time. The feedback control is used to improve the system efficiency, the amplitude of the fundamental voltage and increase the transient response. The system is compared to other approaches and shows an acceptable level of performance as shown in simulation results.

Chapter 2

REVIEW OF CONTROL METHODS

In this chapter we are going to discuss some of the digital, adaptive and learning controllers. Starting by the learning controller, we can state that a learning controller uses prior data to establish a new control signal. These methods of control can be taught from the practice to develop control presentation and diminish the tracking error [4].

2.1 Iterative Learning Control

Iterative Learning Control (ILC) is a control method used to enhance the transient performance of system that work repeatedly for a preset time period, or it could be defined as mentioned in [5]. “The main idea behind ILC is to iteratively find an input sequence such that the output of the system is as close as possible to a desired output. Although ILC is directly associated with control, it is important to note that the end result is that the system has been inverted” [5].

ILC has become an interesting method of control for the reason that simple control configuration and excellent tracking performance. For the systems where ILC controller is used, the system uses the information collected from the earlier implementation of the similar duty repetitively to form the control action for the current operation with the purpose of improving the tracking performance from iteration to iteration, like what happens in robot arm manipulators and assembling tasks [6].

This method of control is especially used to obtain a specified transient response of a system which is operated repetitively. Using such a controller it's possible to obtain ideal tracking, still even if the mode is unknown and there is no a priori information about the system structure. Also this controller is capable of dealing with nonlinear systems [7].

The motivation toward discovering ILC control, firstly is to solve the problems that couldn't be solved using traditional controllers, especially when a desired transient response is required for particular cases for the systems which operate repetitively. Secondly, repeating processes in industrial applications such as robots, which repeat the same mission from test to test, has mainly focused on batched processes. Batched processes are suitable for low/high volume goods which can be defined as follow [4]:

$$x\left(t+1,k\right) = Ax(t,k) + Bu(t,k) + w(t,k) \tag{2. 1}$$

$$y\left(t,k\right) = Cx(t,k) + v(t,k) \tag{2. 2}$$

For $t = 0,1,..........,T-1; k = 1,2,......$

where $x,w \in R^n y,v \in R^m$ and $u \in R^p$. which denote the states, disturbances, output, measurement noise and inputs respectively. A, B and C are the system matrices with suitable size, t represents different time steps, and T is the period of each batch index with primary state $x\left(0,k\right) = x_0$.

If we define the tracking error as:

$$e(t,k) = y_r(t) - y(t,k) \qquad (2.\ 3)$$

Then the aim of the controller is to have $\lim_{x\to\infty} e(t,k) = 0$.

The simplest function for the ILC is:

$$u(t,k) = u(t,k-1) + \mathrm{k}_{ILC} e(t,k-1) \qquad (2.\ 4)$$

Notice that the input of the present batch are specified by the earlier batch in addition to the proportional term (with factor of k_{ILC} called the learning matrix). This type of ILC's is called a P-type ILC controller.

Also ILC can be shown as:

$$u(t,k) = Q_{ILC}\left(u(t,k-1)\right) + r(t,k) \qquad (2.\ 5)$$

such that $Q_{ILC}\left(u(t,k-1)\right)$ called the feed-forward factor for ILC; $r(t,k)$ is called the updating law for ILC; Q_{ILC} is called Q –filter, which improves the robustness of the controller at high frequency disturbance which makes it hard to eliminate the steady state error. The new linear is

$$r(t,k) = \mathbb{L}_{ILC}\left(e(t,k-1)\right) \qquad (2.\ 6)$$

where $\mathbb{L}_{\mathrm{ILC}}$ is called the L-filter.

Generally ILC improves tracking performances after a few iterations by a self tuning process without using the system model. There are many types of ILC controllers. Firstly, the classical algorithm uses feed-forward control and can reduce the tracking error to zero. Secondly, we can classify the types of ILC's according to learning action type as P-type, D-type, PD-type and PID type, and so on. If the current iteration tracking errors were used to figure the control input, this can be viewed as an on-line ILC, then it will be called a D-type online or P-type online ILC controller etc. [6]. The main advantages of ILC controllers can be summarized as:

1. No need for dynamic representation of the control system.
2. Able to reduce the tracking error to zero as the iteration increased.
3. The ability to achieve fast converge rates by selecting high feedback control gain.

2.1.1 ILC Applied to UPS Inverter

It's obvious now that ILC is used where the error signal is periodic, like what we have in nonlinear loads applied to UPS systems, where the controller is reducing the error iteratively. For open loop inverter operation with feed-forward control which forms the main component of the control signal as in [8]. For the inverters due to the presence of the LC filter, a zero phase shift filter is designed and applied to the inverter in order to improve the dynamics of the inverter and to have faster error converges. Because of the open loop nature of this method, a forfeiting factor is established with the purpose of improving the robustness of the inverter.

The method of control is introduced in [9], which introduce a new scheme called *Hybrid ILC* which is the same as ILC introduced in[8], but PD controller is added in parallel to the ILC and the feed-forward reference signal, before comparing the output of the addition to triangular signal. This modification reduced the THD values, faster converge and good steady state error, but still having the disadvantages of complex implementation. This method is suitable for the application of the UPS inverter, where the quality of the steady state output is much important rather that fast response.

2.2 Repetitive Control

Repetitive control method was established depending on the Internal Model Principle [45]. The internal model principle (IMP) proposed by Francis and Wonham, states that if any foreign signal can be regard as the output of an independent system and if this signal is joined to a closed-loop system, then it will guarantee ideal tracking or complete rejection of that system. When this principle is joined with the truth that any cyclic signal with a known time can be established by a time-delay positive feedback system with a suitable initial function, we form the basis of repetitive control theory [10]. RC is commonly used in the systems which deal with periodic signals (for ex. when we want to track periodic reference and when it's required to reject periodic disturbances), as in industrial manipulators executing operations like picking or placing objects [11].

This control method is a straightforward learning method which was established for the reason of simple and straightforward implementation; it's well-known by its high accuracy and independency from the system which it's applied on. RC became a major approach which used extensively in nonstop route for tracking or rejecting foreign signals where the period of the foreign signal is known [10].

To illustrate this method of control let's consider a linear system given by [4]:

$$Y\left(Z^{-1}\right)=G\left(Z^{-1}\right)U\left(Z^{-1}\right) \tag{2. 7}$$

where, Z^{-1} is the backward shift operator; G is the transfer function; Y and U are the z-transforms of outputs and inputs respectively. For any periodic signal with period T, using the system shown in Figure 2.1 and after adjusting the initial parameter of the system, we generate a free time-delay system. Any controller have such a generator is called a repetitive controller. This controller aims to have an output tracking a given trajectory $R(Z^{-1})$ with known period T, such that the tracking error goes to zero while time became very large.

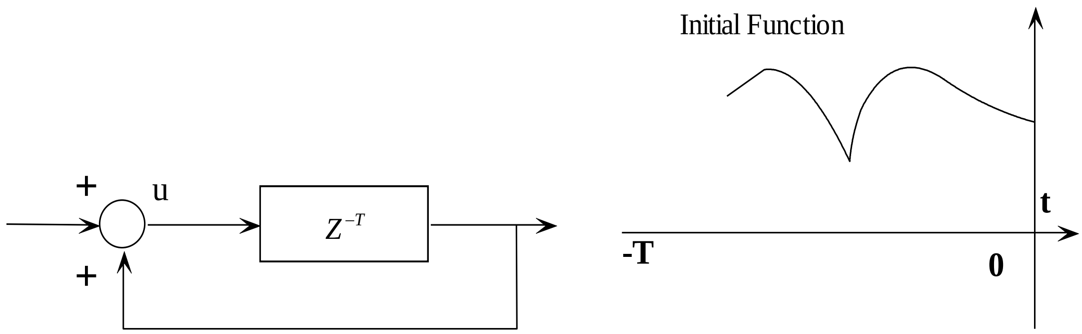

Figure 2.1: Generator of periodic signal [4].

There are many approaches for designing Q and L filters. The design problem is to improve the robustness of the controller. There are many types of RC controllers.

2.2.1 Continuous Time Delay

The first inspiration and envoy example was to control proton synchrotron magnet power supply, particularly because of the complexity of obtaining high control precision using further control approaches [10]. The creativity of the repetitive control is that it has effectively applied a time delay internal model of any periodic signal with period T, which means:

$$M_{Ic} = \frac{1}{1-e^{-TS}} \qquad (2.\ 8)$$

In theory, by including M_{Ic} interested in the feedback loop and keeping it stable, then perfect tracking or complete rejection can be achieved for any periodic signals. Notice that the system which built depend on M_{Ic} controller is infinite dimensional system. Some general design guidelines are presented in [12], [13] and [14], which discuss the frequency domain analysis and synthesis.

2.2.2 Discrete Time Delay

For a discrete time classification, once the sampling period T_s is coordinated with the reference disturbance signals. N is defined as number of sample/period is taken, $T=NT_s$, a discrete periodic signal originator can be selected as:

$$M_{ID} = \frac{1}{1-Z^{-N}} \tag{2. 9}$$

Using this controller steady-state error can be eliminated for all the cyclic waveforms, given that M_{ID} is located in a stabilize closed-loop system. Unlike the continuous time delay, the discrete time delay internal model M_{ID} M_{ID} is finite dimensional.

Advantages of RC can be concluded as follows: high accuracy, straightforward completion and slight dependence on the system parameter (the controller is independent of the system's parameters) [10].

2.2.3 RC Applied to UPS System

In [19, 20] a new approach is introduced that depends on the combination of conventional PI controller and repetitive controller which is applied to UPS Inverter. The basic idea of this approach is that, when the transient error is small the repetitive controller is handling this error and reducing it, and when the error increases to large values due to disturbances, a PI controller is used efficiently to reduce the error by choosing a large value of the proportional term. Note that the integral term should also be chosen carefully. In [19] a simple implementation of this approach is presented, which reveals on zero steady state error at the output. While in [20] a modified approach using “saber” is introduced with a comparison with the traditional repetitive controller.

In [21] a control method which introduces both pole assignment and repetitive control together working to have an acceptable steady state error in the application of UPS inverters. Choosing the observer poles to be 2-3 times further from the system poles, a small steady state error can be achieved. By plugging in a repetitive controller which deals periodically with the errors, steady state error can be reduced furthermore.

By combining SVPWM with repetitive controller a high quality output with reduced cost can be achieved. This approach is suitable for the application where the product response is not that important as much the quality of the output signal. A zero phase shift *notch filter* is used to eliminate the resonant peak of the inverter. The notch filter provides a wide range to parameters variation, and much better harmonic rejection with fast error converges is achieved using this approach, which is a cost effective approach applied to UPS inverters.

2.3 Deadbeat Control

Deadbeat control is a discrete control method which aims to find appropriate input signal to be applied to a system such that we have zero error at the output at the steady state in a minimum number of time steps with zero initial condition.

Noticing that for an Nth order system these steps could be at maximum N, which means that the system in not controllable, so the problem could be solved by applying a feedback loop with specified parameter values in order to ensure that the new poles of the transfer function are at the origin of the z-plane.

If we assume that we have a stable plant without dead-time, with a unit step input, noticing that while the difficulty but it's still possible to design a controller for unstable plants without unit step input [23]. Usually, design process is executed in three steps. Firstly, the controller will maintain the fastest response when the output signal is established in one sampling step. The control signal caused by this step is very high, and in most cases the oscillation will occur near the sampling points. This oscillation is caused by cancelation of the zeros of the transfer function outside the unit circle in the z-domain. Secondly, the design is modified to avoid the oscillations that occur in the first step. Zeros of the transfer function is divided into cancellable which will appear in the controller function, and the second ones are the non-cancellable zeros [23].

Further modification could be applied to the system if the control signal is still high, but this will increase the settling time again if you are going to use the polynomial algorithm as a refining solution for the system. Notice that, the design is executed in the s-domain, which is a very interesting feature here because it eliminates the undesirable oscillation and there will be no too high control signal like what we have in time domain frame[23]. For understanding the problem let's consider a linear system given as,

$$X_{K+1} = Fx_k + Gu_k \quad (2.\ 10)$$

where $u_k \in R^m$ and $x_k \in R^n$. The aim of the controller is to find a feedback gain given as:

$$U_K = -L_{Xk} \quad (2.\ 11)$$

This moves all the initial values of the system to the origin with minimum step number.

There are many approaches to solve this problem such as Quadratic Function solution, State Space solution, Liner Quadratic Regulators and Pole Placement solution which will be discussed here [22].

2.3.1 Pole Placement Control

Here we will discuss how to make the closed-loop system a second order system with a preselected delay. By applying the following design procedure we can design a selected values for rising time, settling time and over/under shoot such that the stability of the system is achieved. Here second degree of freedom (2-DOF) is discussed while the noise effect is ignored [24].

Let us begin with the plan

$$Y(z) = G(z)U(z) \quad (2.\ 12)$$

With transfer function

$$G(z) = z^{-1}\frac{B(z)}{A(z)} \quad (2.13)$$

where B(z) and A(z) are co-prime (i.e.: A and B have no common factor). The aim is to design a controller such that the output signal Y is in relation with the preselected value and affected by the control signal r.

2.3.2 Deadbeat Control Applied to UPS Inverters

In [25-27] the two poles of the system are placed in the feedback, one placed at the origin which represents the output voltage, and the other one having magnitude considerably less than unity which represents the capacitor current. The response of the output voltage is considerably accepted, but because the response of the current cause high electromagnetic interface (EM); the overall efficiency of the UPS system is noticeably reduced.

In [28], by using delay in the treated inverter voltage with small delay in the sampling period while the earlier voltage applied to the inverter is kept for the next step, the problem of te computation delay had been eliminated.. Using this method the processor will have more time for computation operation and the delay will be much smaller and the implementation will be simpler.

Deadbeat control aims to locate the poles of the system at the origin, this implies that the load voltage should follow the reference voltage within acceptable range; this means that the transient response to nonlinear load (e.g. triac load) is much faster. One more advantage of this approach that steady state performance is improved. But there is still big under shot in the load voltage with non liner loads.

Finally the main properties of the deadbeat control method are that deadbeat response has zero steady state error, with minimum rising/settling times and small overshoot/undershoot at the output signal which reduce the distortion and improve the quality of the inverter.

In [29] parallel operation of UPS inverters is introduced. Because of the fast dynamic response and high quality of a modified deadbeat controller with proportional term plugged in the controller, which improves the robustness of the traditional dead beat. Synchronization of the output waveforms is applied to the system, and the average load sharing is considered.

Five different control methods were introduced in [30], all of these controllers are using deadbeat control applied to UPS inverters, and using Field Programmable Gate Array (FPGA) based hardware. A comparison between the introduced methods was introduced, which shows that the controller had very good transient response.

2.4 Adaptive Control

Adaptive control is a technique applied in dynamical systems which have constant or slowly-varying uncertain parameters, such as robot manipulators which can carry large objects with unknown initial weights. The point of adaptive control is how to guess these unknown variables on-line based on the measured system signal. So it’s an on-line estimator controller. Adaptive control is used when we are dealing with complex systems with unknown parameters, such as UPS Inverters.

There are two main approaches for the implementation of adaptive control. First of them is model reference adaptive controller, and the other one is self-tuning controller [31].

2.4.1 Model Reference Adaptive Control (MRAC)

MRAC consists of four main components, starting with the plants which are assumed to have known structure with unknown parameters. Secondly, a reference model which determines the best response of the controller, the output of which is subtracted from the output signal Y to define an error. Noticing that choosing the reference value is part of the controller design, the third component is the controller which contains a number of adjustable parameters with the goal to have perfect tracking capability. Finally we have the adaptation mechanism which is used to modify the parameters in the control law in order to reduce/ eliminate the error.

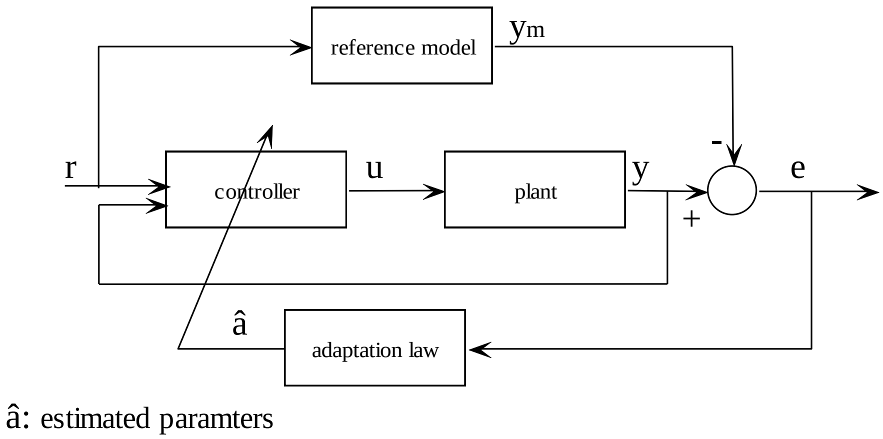

Figure 2.2: Model Reference Adaptive Controller [31].

The main feature of MRAC shown in Figure 2.5 is that the design of this controller must be chosen carefully such that the output, the reference and the control signals are determined to have zero steady state error. If not, we will have an improper control signal which will give an unacceptable output signal.

2.4.2 Self Tuning Controllers (STC)

The structure of STC is suitable for stochastic processes where the output is initially estimated when the plant parameters are unknown. Figure 2.5 shows the main features of this method.

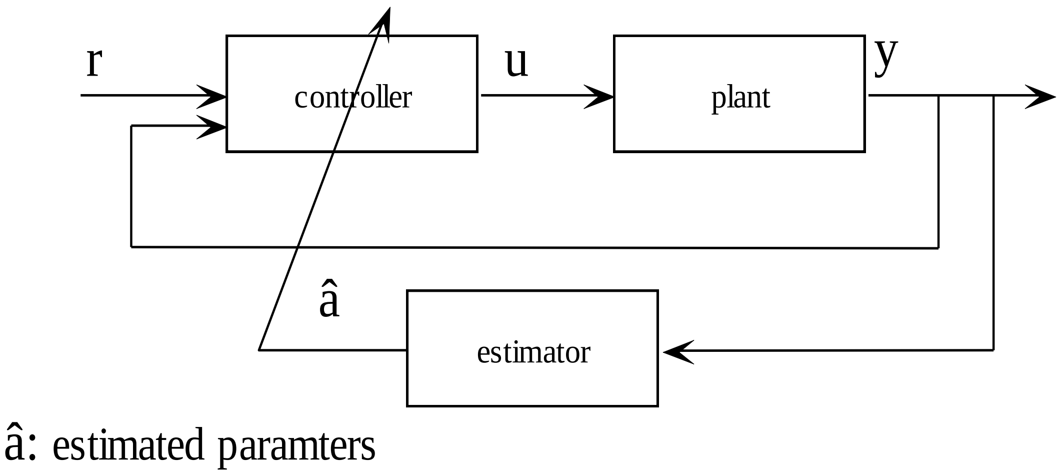

Figure 2.3: A self tuning adaptive controller [31].

At each time step, a set of estimated plant values â are sent to the controller, which is calculated depending on the previous plant input u and output y, and the controller finds the new value of u depending on the control and measured signals, which will give a new output y again. This routine will be continuously repeated and because of this nature it is called an adaptive controller.

Finally, a comparison between robust control and adaptive control is made in [32]. In principle, adaptive control is higher level and more efficient than robust control when we are dealing with unknown parameters. Because of the learning nature of adaptive control, which adapts or learns as time goes on, this controller improves its efficiency and adapts itself to the new circumstances, while robust control tries to keep system robust against changes occurring to the system. One more reason that shows the learning behavior of adaptive control is that adaptive control does not need (or needs little) a priori information about the unknown parameters. At the same time one of the most interesting features of robust control is that it can handle the disturbance to the system by changing the parameters of the system, which means having very fast response.

In other words, robust control ensures that if the uncertain parameters are within specified bounds, then the control law will not change while adaptive control changes the control law adaptively. It's possible to combine both robust and adaptive control to have what is called robust adaptive control.

There are many schemes which vary from the basic block shown in Figure 2.7. The difference may occur in the performance measurement, comparison-decision, or in the adaptation mechanism [33].

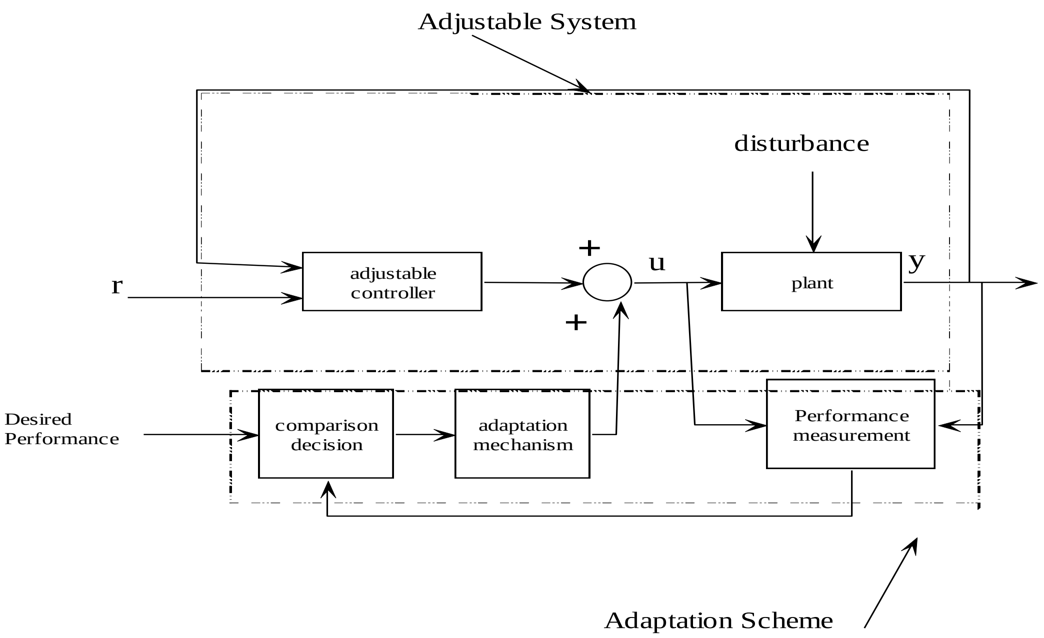

Figure 2.4: General structure for adaptive control [33].

The main property which makes one distinguish between an adaptive controller and the others is the fact that adaptive control uses the information collected in real time to achieve a desired performance (i.e. feedback technique may be proposed). While it's possible to achieve a level of desired performance using a fixed controller where the system is affected by disturbances, like what we have in robust control, still such a controller is not adaptive. Open-Loop Adaptive Control, Direct and/or indirect Adaptive Control, Adaptive Regulation, Adaptive Feed forward Compensation of Disturbances and others are some examples for schemes used in adaptive control [33].

2.4.3 Adaptive Control Applied to UPS Inverter

Generally, adaptive control is used for the application where a high performance UPS inverter for ac power supply is required, which is the case of [30, 34 and 34]. In[30], both repetitive and adaptive control are combined together, which gives a controller capable of eliminate periodic waveform distortion, without any *priori* of the plant parameters.

In [34], a recursive real time least square estimator is has been used in order to estimate the system dynamics. Simulation shows that the controller has an advantage over the conventional repetitive controller, its guarantees the system's stability and it's robustness against system variations. While in [35] a new digital adaptive controller is introduced, where the cost of the gain function of the tracking error and the control signal is reduced in order to reduce the total harmonic distortion. At the same time, the controller keep the robustness of the system to an a acceptable level. Moreover it can be designed to uncertain parameter (i.e. without any *priori* knowledge about the system's parameters).

Chapter 3

SLIDING MODE CONTROL BACKGROUND

3.1 Basic Notion of VSC

A clear understanding of SMC can be demonstrated by an example which could be found in [36, 37]. Here two examples will be presented, as follow:

$$\begin{bmatrix} \dot{x}_1 \\ \dot{x}_2 \end{bmatrix} = \begin{bmatrix} 0 & 1 \\ -1 & 2 \end{bmatrix} \begin{bmatrix} x_1 \\ x_2 \end{bmatrix} + \begin{bmatrix} 0 \\ 1 \end{bmatrix} u \qquad (3.1)$$

where

$$u = \psi x_1$$

$$\psi = \begin{cases} -4, s(x_1, x_2) > 0 \\ 4, s(x_1, x_2) < 0 \end{cases} \qquad (3.2)$$

and

$$s(x_1, x_2) = x_1 \sigma \ , \qquad \sigma = 0.5x_1 + x_2 \qquad (3.3)$$

The block diagram shown in Fig. 3.1 represents the system given by (3.2). The equation $s(x_1, x_2) = 0$ defines the regions on the state plane where $s(x_1, x_2)$ has different signs. This equation can also be written as

$$x_1 = 0 \quad \text{and} \quad \sigma = 0.5x_1 + x_2 = 0 \qquad (3.4)$$

Equation (3.4) corresponds to lines on the state plane, shown in fig 3.2, and are called *switching lines,* which divide the state space into many regions such that the function $s(x_1, x_2)$ has different sign in each region. The function $s(x_1, x_2)$ is called a *switching function*, and the set of points defined by $s(x_1, x_2) = 0$ $s(x_1, x_2) = 0$ is called a *switching surface* or *sliding plane.*

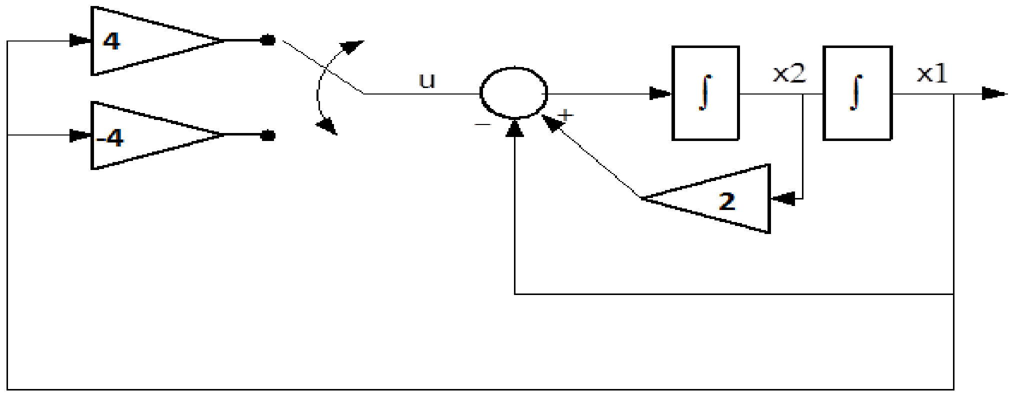

Figure 3.1: Model system for the given example of VSC [37].

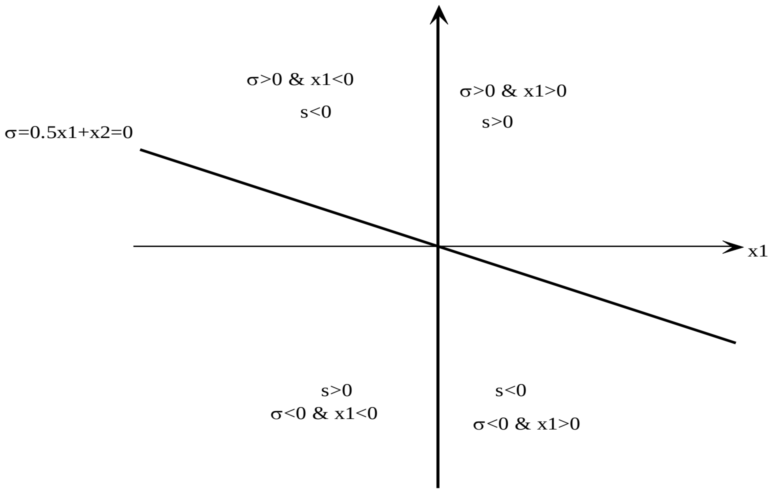

Figure 3.2: Switching regions which defined by switching logic [37].

Because of the feedback gain ψ the behavior of the system will change accordingly, and the phase plane will be divided into two regions as follows:

- When $s(x_1, x_2) > 0$,

$$\dot{x_1} = x_2$$

$$\dot{x_2} = -x_1 + 2x_2 - 4x_1 = -5x_1 + 2x_2 \qquad (3.5)$$

If we transform the system to matrix form given by $\dot{x} = Ax$ then

$$A = \begin{bmatrix} 0 & 1 \\ -5 & 2 \end{bmatrix},$$

Which has complex conjugate eigenvalues with positive real parts $(1 + 2i\ , 1 - 2i)$. The resultant phase plane trajectories are shown in fig 3.3, which spiral outward from the equilibrium point (0,0), which is therefore unstable

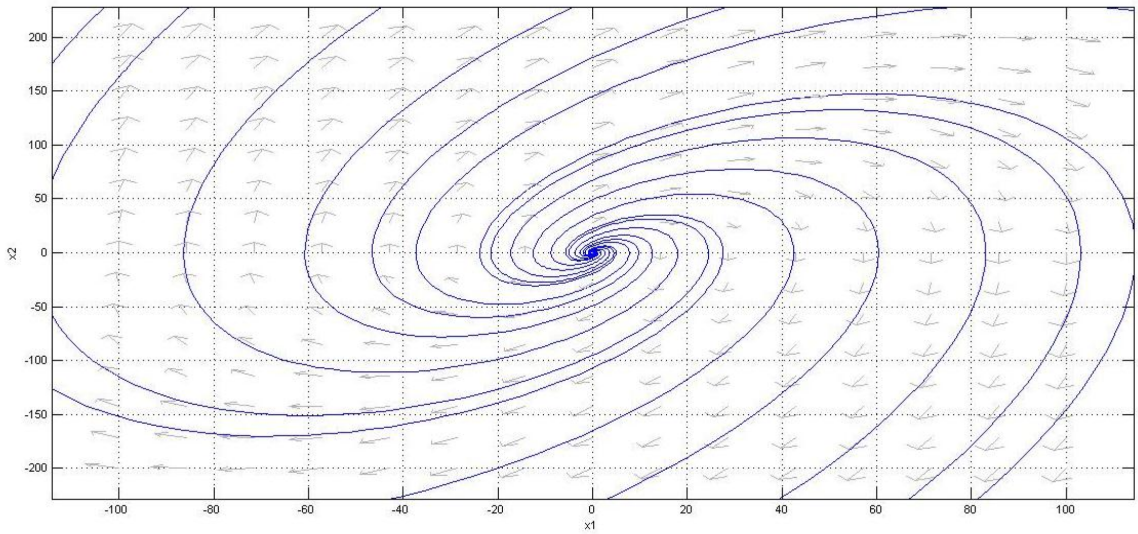

Figure 3.3: The phase portrait of the system when $s(x_1, x_2) > 0$ [37].

- when $s(x_1, x_2\,) < 0$,

$$\dot{x_1} = x_2$$

$$\dot{x_2} = -x_1 + 2x_2 + 4x_1 = 3x_1 + 2x_2 \qquad (3.6)$$

Then the matrix

$$A = \begin{bmatrix} 0 & 1 \\ 3 & 2 \end{bmatrix},$$

which has two distinct real eigenvalues with opposite signs (-1,3). This type of critical point is called a saddle point, which is always unstable. Figure 3.4 shows it’s phase portrait.

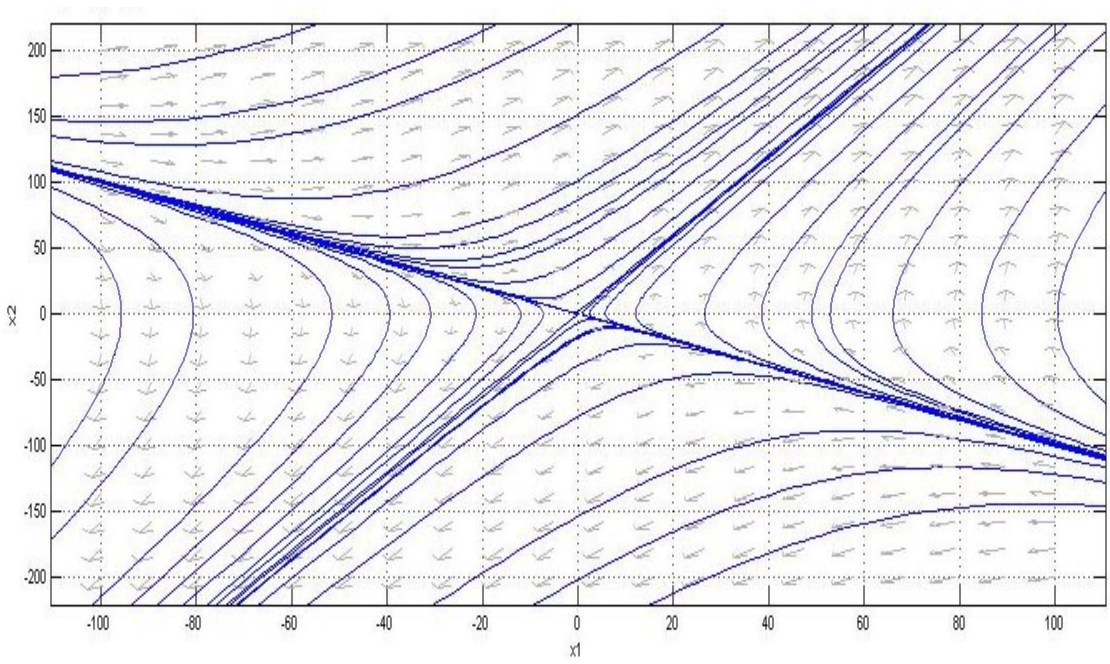

Figure 3.4: The phase portrait of the system when $s(x_1, x_2) < 0$ [37]

Referring to Figure 3.5 we notice that the state trajectory moves toward a specific switching line $\sigma = 0$, while the line $x_1 = 0$ doesn't affect any motion occurring on the state plane, and does not cause any unusual motion to there. The switching line $x_1 = -0.5\, x_2$ or equivalent ($\sigma = 0$) is a line on which all the other trajectories from both sides end. This interesting line is called a *sliding line* and the movement of all the points on it towards the origin (steady state point) is called the *sliding mode*, as the states "slide" on the sliding line before reaching the equilibrium point at (0, 0) on the phase plane. Equivalently, the movement of the state from any point toward the sliding line in a finite time is called the *reaching mode* [37].

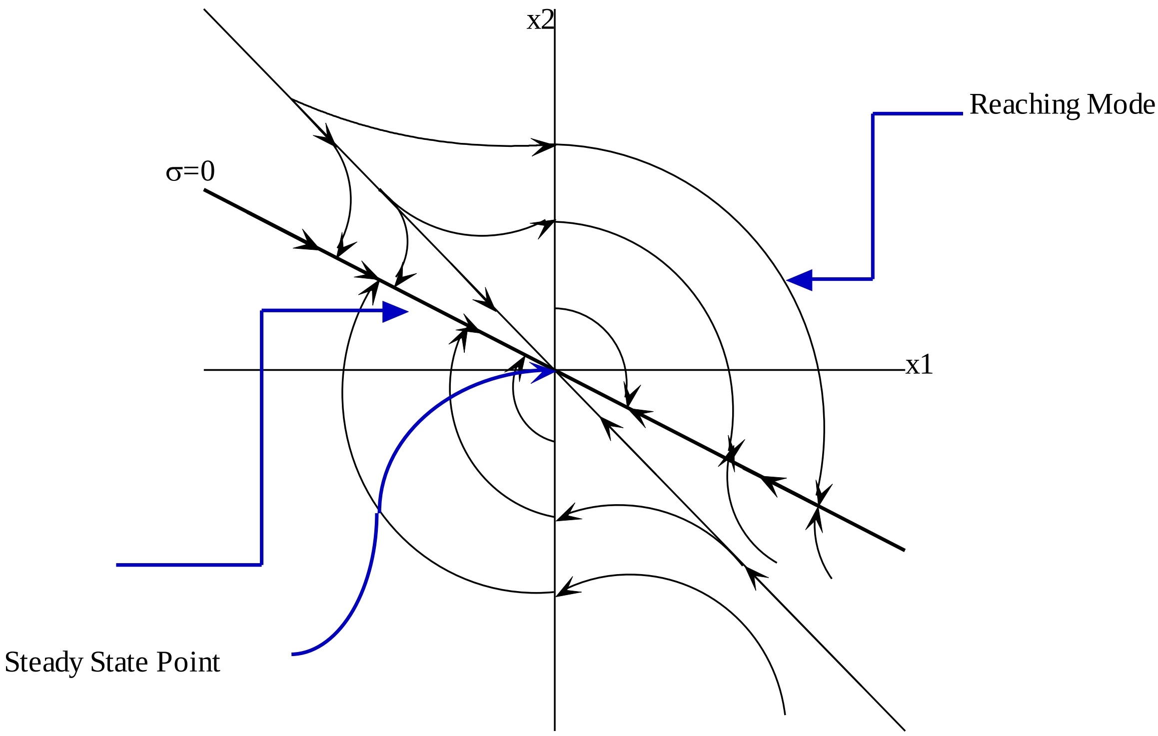

Figure 3.5: Trajectory of the system given by equation (3.1) [37].

So, for all the time the structure of the equation (3.1) consists of both structures of the system described by (3.5) and (3.6). The system undergoes through different modes which are the reaching mode, the sliding mode and the steady state mode.

The system is called *variable structure* (VSC) because of the existence of the feedback control law which alternates from one form to another. The structure of the control law varies depending on the position on the control law (for instance -4 and 4 in the given example) under very fast speed. High switching frequency is one of the main interesting properties of Variable Structure Control Systems [11].

3.2 Statement of Variable Structure Control

In this section we are going to state the problem of VSC in a general form, for a system given by [37]

$$\dot{x} = A(x,t) + B(x,t)u \tag{3.7}$$

where dim- **x** =n and dim-**u** =m.

The design problem, firstly, is to find m switching functions which are expressed by the vector switching functions(x). This means that we have to design a switching surface $s(x) = 0$ to express a system which is lower order from the original one,(i.e. with dimension (n-1)). Secondly we have to find a variable structure control input u given by:

$$u = \begin{cases} u^{+}(x,t) & ,s(x) > 0 \\ u^{-}(x,t) & ,s(x) < 0 \end{cases} \tag{3.8}$$

The control input u must ensure that from any point of the state space, the trajectory of the manifold must be directed toward the switching surface $s(x) = 0$ in finite time. This means that u must be designed to make the reaching mode satisfy the reaching condition.

3.3 VSC Applied to Linear Systems

Consider the linear system given by (3.7). For this system

$$\dot{x_1} = A_{11}x_1 + A_{12}x_2 \tag{3.9}$$

$$\dot{x_2} = A_{12}x_1 + A_{21}x_2 + B_2u$$

Where $A_{ij}(i, j = 1, 2)$, and B_2 are constant matrices, has appropriate dimensions (det $B_2 \neq 0$) [38] . Both A and B are constant matrices, $x_1 \in \mathbb{R}^{n-m}$,and $x_2 \in \mathbb{R}^{m}$. If we assume that the sliding surface is given by

$$s = Cx_1 + x_2, \quad s \in \mathbb{R}^{m} \tag{3.10}$$

If we apply the same steps as in the previous example, we notice that the sliding surface will be given as $s = 0$ which is the same as $x_2 = -Cx_1$, and the system has order (n-m) (R^{n-m}), given by:

$$\dot{x_1} = (A_{11} - A_{12}C)x_1 \tag{3.11}$$

It's possible to achieve the required dynamic properties by placing (locating) the eigenvalues of the closed loop system with linear feedback. This can be achieved by a conventional control method, (e.g. PID or Pole Placement control). But the new thing which is represented in the theory of sliding mode control is that, the control input will be one step degree lower than the controlled system.

So the order of equation (3.11) is decreased by a quantity which is the same as the control dimension. For system (3.7) there exists a matrix C, which can achieve the required and suitable eigenvalues of the system, so that the system has the required dynamic properties (see [39], [40] and [41] for more detail). The matrix C became a solution for (n-m)th order for "a new" system and responsible of determining the eigenvalues of (3.11).

Continuing with the former example, the next step of sliding mode control is to determine the equation which ensures the discontinuity property for the system, and which ensures that the entire manifold will move toward the sliding line $s = 0$. The motion on the sliding space is described by:

$$\dot{s} = Rx + B_2u \tag{3.12}$$

$$Rx = (CA_{11} + A_{21})x_1 + (CA_{12} + A_{22})x_2 \tag{3.13}$$

If we choose the discontinuous control to be

$$u = -a|x|{B_2}^{-1}\, sign(s) \tag{3.14}$$

where a is a constant, and $|x|$ represents the sum of absolute values of vector x components. Then

$$\dot{s} = Rx - a|x|\, sign(s) \tag{3.15}$$

This equation states that there exists a positive value a**,** which will ensure that both of the functions $\dot{s}$ and s have different signs at the same time (i.e. the sliding mode will take place at each discontinuity surface).

3.4 Reaching Condition and Reaching Mode:

3.4.1 Reaching Condition

Reaching mode is the interval where the entire state moves toward the sliding line. This could be achieved by stating the following conditions, which are called the reaching conditions:

$$\dot{s}_i < 0 \quad when \quad s_i > 0 \tag{3.16}$$

$$\dot{s}_i > 0 \quad when \quad s_i < 0 \tag{3.17}$$

This means that, "the entire individual switching manifolds and their intersections are all sliding manifolds" [42]. These conditions can be represented as

$$s^T s < 0 \tag{3.18}$$

This means that only the joint of all switching manifolds is the sliding manifold [42].

3.4.2 Reaching Law

This is established by a differential equation representing the dynamic of the switching function [37]. The behavior of the dynamic system can be improved by adjusting the parameters of the differential equation. A general form of reaching law is given by:

$$\dot{s} = -Q\ \mathrm{sgn}(s) - \mathrm{K}\ \mathrm{h}(s) \tag{3.19}$$

Where

$$Q = \mathrm{diag}[\, q_1 \ , \dots \dots , q_m \,], \quad q_i > 0$$

$$\mathrm{sgn}(s) = [\, \mathrm{sgn}(s_1), \dots \dots , \mathrm{sgn}(s_m)]^T$$

$$K = \mathrm{diag}[k_1 \dots \dots , k_m], \ \ k_i > 0$$

$$h(s) = [h_1(s_1), \dots \dots , h_m(s_m)]^T$$

$$s_i h_i(s_i) > 0 \qquad h_i(0) = 0$$

There are many approaches for reaching law:

A- Constant rate reaching: which is given by:

$$\dot{s} = -Q\, sgn(s) \tag{3.20}$$

This law forces s(x) to reach the switching line s=0 at constant speed. If q_i is too small, the reaching time will increase, and if q_i is too large this law cause chattering.

B- Constant plus proportional control law, which is given by:

$$\dot{s_i} = -k_i\, |s_i|^{\alpha}\, sgn(s_i) \tag{3.21}$$

This law is a modification of the previous one, which forces the state variable to arrive at the sliding manifold faster by adding the proportional term.

C- Power rate reaching law, which is given by:

$$\dot{s} = -Q\, sgn(s) - K\, h(s) \tag{3.22}$$

This will boost the speed when the state variable is away from the switching line, and will decrease it when the state variable becomes close to the sliding surface. It has advantages of fast reaching time and low chattering.

3.5 Sliding Condition and Sliding Mode

When the phase trajectories move toward the switching line which is given by equations (3.3) or (3.10), this mode is discussed before and is known as the reaching mode. When the trajectory reaches the line and start moving toward the equilibrium point, this mode is called *sliding mode*. The equation $cx = 0$ determines the behavior of the VSS when it's already on the sliding line, and the dynamics depend on the value of the parameter c [24].

A sliding mode exist, if both

$$lim_{s\to -_0}\dot{s} > 0 \;\; and \quad lim_{s\to +_0}\dot{s} < 0 \tag{3.23}$$

are satisfied [37]. Existence of a sliding mode need stability of the state trajectory on the sliding surface $\mathrm{s(x)} = 0$, at least in a neighborhood of $\{\mathrm{x}|_{\mathrm{s(x)}=0}\}$. Geometrically, this implies that the tangent or time derivative of the state vector is pointed toward the sliding surface [36].

3.6 Chattering Problem

As mentioned before, high switching frequency is one of the main characteristics of SMC, because of the nature of the control switch. Practically it's impossible to achieve high switching frequency which is the nature of VSS, because firstly of the presence of time delay in control computation and secondly, because of the limitation of physical actuators, (e.g. when we are controlling a DC servomotor, which has winding inductance, and because it's assumed that the plant input is current, it's impossible to have infinite switching frequency. Here, chattering phenomena appear) [37].

Chattering always appears in the steady state of a VSC systems as a high frequency oscillation around the equilibrium point. This oscillation may excite or motivate other parameters in the systems, which may make the system unstable. Chattering is an undesired phenomena because it reduces control efficiency, heating the switching drive and causing vibration of mechanical parts [38]. There are many approaches to reducing the effect of chattering, considered in the following sections.

3.6.1 The Continuous Approach

Referring to equations (3.2) and (3.8) we notice that the control has a "relay" like nature. Figure 3.6 shows an ideal relay with switching at s=0, which is impossible to implement (i.e. it's not possible to switch between -1 and 1 in zero time).

Regularization of the relay consists of introducing a boundary layer $\|s\| < \Delta$ around the manifold $s = 0$ where the ideal relay will be somehow possible to implement using some close approximation, such that the state trajectory for the system will run arbitrarily (chatter) within Δ [38].

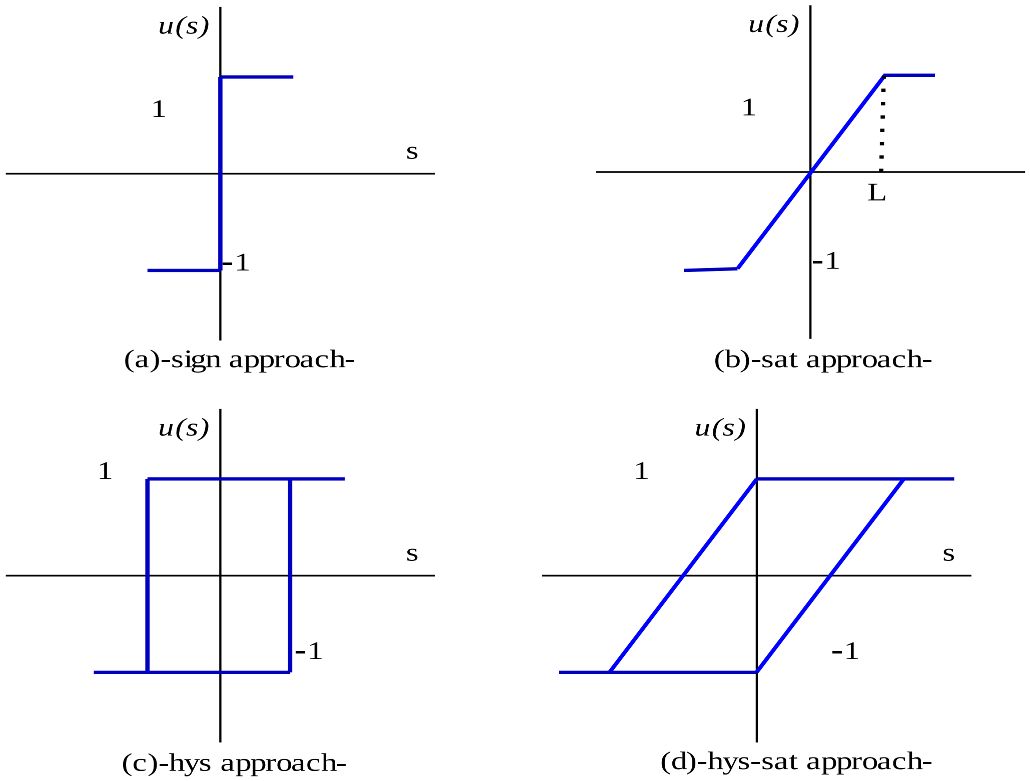

Figure 3.6: Many approaches for designing the relay control [38].

Depending on the previous definition many approaches have been introduced as shown in Figure 3.6, summarized as:

a. The ideal relay control: the control given as:

$$u(s) = \mathrm{sgn}(s) = \begin{cases} +1, & s > 0 \\ -1, & s < 0 \end{cases} \tag{3.24}$$

And shown in Figure 3.6.(a). If this relay is implemented, it will give exact trajectory for the system, and the ideal sliding mode exists on $s = 0$, which means there will be no chattering, and the steady state error is zero.

b. *The ideal saturation control*: which is given by:

$$u(s) = \mathrm{sat}(s) = \begin{cases} +1 \ \text{ when } s > L \\ \frac{s}{L} \text{when } |s| \ \leq L \\ -1 \ \text{ when } s < -L \end{cases} \tag{3.25}$$

Where L is positive, which defines the threshold of the boundary, as shown in Figure 3.6. (b). The state trajectory outside the boundary will be the same as that for ideal relay, and within the boundary it will be forced to follow the line $s = 0$, so it will be also nearly the same as the exact phase portrait of the system. So, the sliding mode does not exist, and of course no chattering occurs within the boundary, and the steady state error is zero if there is no disturbance.

c. *The practical relay control:* shown in Figure 3.6. (c),and given by:

$$u(s) = hys(s) = \begin{cases} +1 \ \ when,\ \ s > \Delta \ or \ (\dot{s} < 0 \ and \ |s| < \Delta\,) \\ -1 \ \ when,\ \ s < \Delta \ or \ (\dot{s} > 0 \ and \ |s| < \Delta\,) \end{cases} \quad (3.26)$$

Where hysteresis width is given by 2Δ. The hysteresis makes the switching possible within $\pm\Delta$ .The phase portrait of the system will be close to the ideal one if the hysteresis is narrow, and there will always be chattering on the existing sliding mode. The system is almost stable, and the origin is not its equilibrium point.

d. *The practical saturation control:* shown in Figure 3.6. (d) which also has hysteresis in its control input. Studying of the behavior of such a controller is complex, because the sliding mode will be eliminated completely, and there will be no chattering at all. The system will be stable at two equilibrium points.

3.6.2 Tuning the Reaching Law Approach

The constant-plus-proportional-rate reaching law is given by

$$\dot{s}_i = \ -q_i \ sgn(s_i) - k_i s_i \quad\ \ for \ i = 1, .., m$$

It's possible to reduce chattering by reducing the parameters q_i and k_i. When the switching function becomes close to zero ($s_i \cong 0$), then$|\dot{s}_1| \cong q_i$. So, by reducing the value of q_i (q_i should not be equal to zero, otherwise the reaching mode will be infinite) the value of the switching function will be reduced when it gets closer to zero (i.e. reduce the chattering). Choosing a large value of k will increase the reaching speed when the state is away from the switching surface.

Chapter 4

SMC OF SINGLE PHASE UPS INVERTER

4.1 Problem Formulation

In this section we investigate the application of sliding mode control theory to the output voltage control of UPS inverters. Figure 4.1 shows a single-phase UPS inverter,

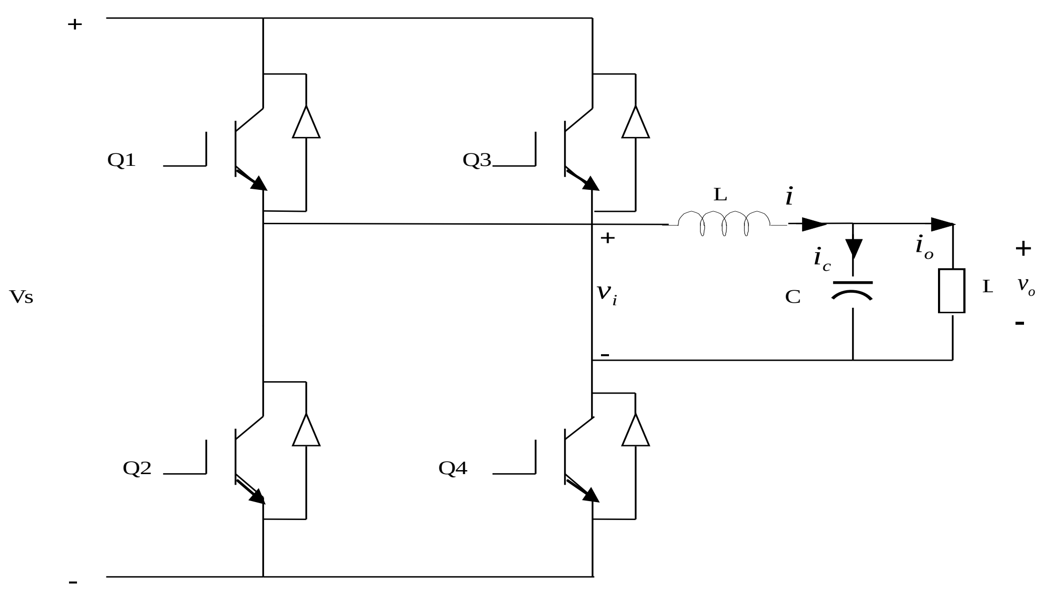

Figure 4.1: Single phase UPS inverter.

The mathematical equations which represent the operation of the inverter are given [43]

$$L\frac{di}{dt} = v_i - v_o \tag{4. 1}$$

$$i = i_c + i_o \tag{4. 2}$$

where $v_i = uV_s$ represents the inverter output voltage, and *u* is the control input function. Now defining the output voltage error x_1 as $x_1 = v_o - v_o^*$, and its rate of change x_2, which is given by its derivative as $x_2 = \dot{v}_o - \dot{v}_o^*$, then (4.1) and (4.2) can be written as

$$\dot{x}_1 = x_2 \tag{4. 3}$$

$$\dot{x}_2 = \ddot{x}_1 = \ddot{v}_o - \ddot{v}_o^* \tag{4. 4}$$

In order to find $\ddot{v}_o$, (4.2) is differentiated as

$$\frac{di}{dt} = \frac{di_c}{dt} + \frac{di_o}{dt}$$

Using $i_c = C\dot{v}_o$, we obtain

$$\ddot{v}_o = [\frac{uV_s}{CL} - \frac{v_o}{CL}] - \frac{1}{C}\frac{di_o}{dt} - \ddot{v}_o^*] \tag{4. 5}$$

Equation (4.5) could be simplified as

$$\dot{x}_2 = w_o^{\ 2}[-x_1 + uV_s + DV_s] \tag{4. 6}$$

The term *D* represents the disturbance applied to the UPS. The controller should show enough robustness against *D*, meaning that the controller should keep the system giving the required output even at the moment when a sudden disturbance occurs. The more the controller is able to maintain the system operating with an acceptable output, the more robust it is. *D* is given by

$$D = -[\frac{L}{V_s}\frac{di_o}{dt} + \frac{v_o^*}{V_s} + \frac{LC}{V_s}\frac{dv_o^*}{dt}] \tag{4. 7}$$

4.2 Norm of the Error Design

In this thesis the sliding surface, defined as

$$s = \lambda x_1 + x_2 \tag{4. 8}$$

is designed such that λ is a nonlinear function of the error norm, as shown in Fig.(4.2). In the interval between e_1 and e_2 on the linear part of the $\lambda - \|x\|$ characteristics

$$\lambda = \beta x_n \tag{4. 9}$$

where β is the slope of the linear part of the λ function. In (4.9) x_n is the norm of the error, represented by x_1 and x_2 as

$$x_n = \|x\| = \sqrt{x_1^{\,2} + \gamma x_2^{\,2}} \tag{4. 10}$$

where, γ is a parameter suitably chosen to ensure that the two terms under the square-root have the same physical unit and are comparable in magnitude.

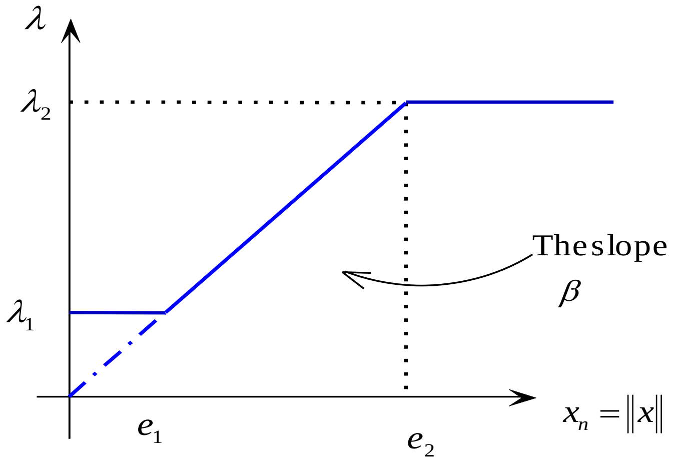

Figure 4.2: The proposed nonlinear function in terms of error norm.

By squaring both sides of (4.9), substituting in (4.10) and solving for x_n yields

$$x_n = \frac{|x_1|}{\sqrt{(1-\gamma\beta^2 x_1^{\ 2})}} \tag{4. 11}$$

During the sliding mode when $s = 0$, we obtain the following equation which describes the dynamics of the output voltage error

$$\dot{x}_1 = x_2 = -\lambda x_1 = -\frac{\beta x_1^{\ 2}\,\mathrm{sgn}(x_1)}{(1-\gamma\beta^2 x_1^{\ 2})^{1/2}} \tag{4. 12}$$

Notice that if $x_1 < 0$, then (4.12) becomes

$$x_2 = \frac{\beta x_1^{\ 2}}{(1-\gamma\beta^2 x_1^{\ 2})^{1/2}} \tag{4. 13}$$

Notice that the denominator of (4.13) should always be positive, so that the system always has a solution (see appendix A for the proof of this fact). For solving (4.12) the following integration has been used (see appendix A for more detail),

$$\int \frac{(1-ax_1^{\ 2})^{1/2}}{x_1^{\ 2}} dx_1 = -[\frac{\sqrt{1-ax_1^{\ 2}}}{x_1} + \sqrt{a}\sin^{-1}(\sqrt{a}x)] \tag{4. 14}$$

Then, (4.12) can be solved as

$$\Delta t = (t_2 - t_1) = \frac{\mathrm{sgn}(x_{11})}{\lambda_2} - \frac{\mathrm{sgn}(x_{12})}{\lambda_1} + \frac{1}{\beta}\sin^{-1}\left\{\frac{\sqrt{\gamma}(\lambda_2-\lambda_1)}{[(1+\gamma\lambda_2^{\ 2})(1+\gamma\lambda_1^{\ 2})]^{1/2}}\right\} \tag{4. 15}$$

where x_{11} represents the initial value of the error voltage when the state trajectory starts to slide on the line $s = 0$, and x_{12} represents its final value, while Δt represents the time needed to slide from x_{11} to reach x_{12} as shown in Figure 4.3.

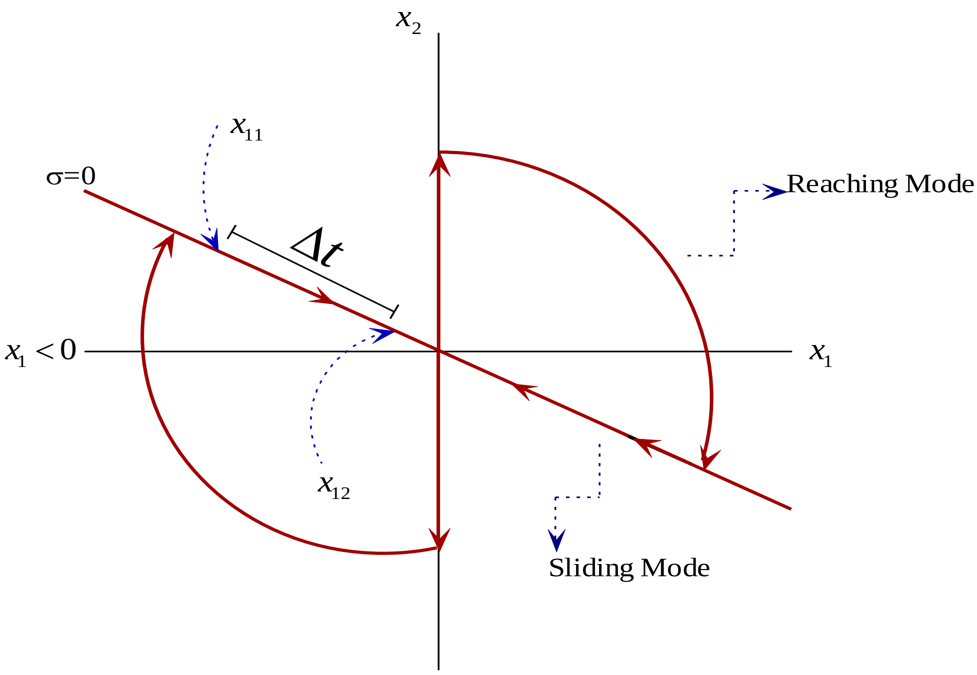

Figure 4.3: x_{11}, x_{12} and Δt on the state plane.

The aim is to reduce the sliding time as much as possible, such that the controller returns the system to the origin when a disturbance is applied to the system. Figure 4.4 shows the graph of β, γ and time, for fixed value of β and by varying γ. MATLAB implementation of the proposed method is given in appendix B, and the triggering signals are shown in appendix C.

4.3 Parameter Choice

For any design issue, parameters choosing are an important issue. Here we choose the parameters such that a minimum steady state error achieved at fast response. Choice of γ depends on Figure 4.4 above, to the extreme minimum, with value of 1×10^{-36} and beta was chosen with value of 1×10^{4}.

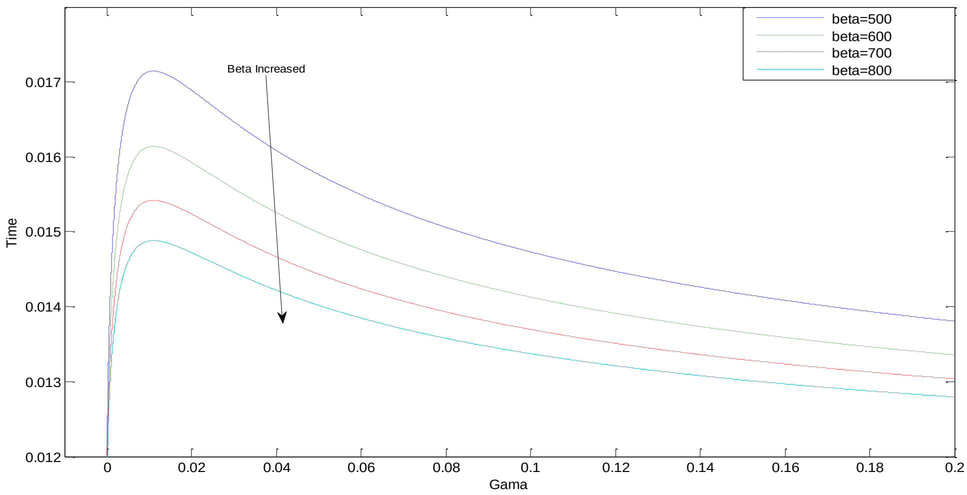

Figure 4.4: γ vs. time for fixed value of β .

The above figure is plotted for gamma between (0-0.2) and for many values of beta 500, 600, 700 and 800 alternatively. Appendix D shows the MATLAB m-file for plotting Figure 4.4 depending on equation (4.15).

Chapter 5

COMPUTER SIMULATIONS

5.1 Introduction

In this chapter we introduce and discuss simulation results for various SMC approaches applied to single-phase UPS inverters. All of the approaches are discussed under the same conditions. A triac-controlled resistive load ($R = 3\Omega$) with firing angle 90° simulates a sudden disturbance occurring on the load side. Another disturbance is created by a full bridge diode rectifier connected to a $400\mu F$ capacitor in parallel with a 60Ω resistor.

Firstly, we introduce a three-level hysteresis function approach [43], which uses the three-level sliding function directly to control the switches of the inverter. The switching function is ON during one half cycle only, while turned ON or OFF during the other half cycle, so the switching frequency is half of that in the traditional form of three-level hysteresis control.

Secondly, we discuss the rotating sliding line approach [44], which introduces the possibility of rotating the time-varying sliding line, such that the tracking time of the output voltage during the disturbance is improved. The function which is used to rotate the sliding line is derived from fuzzy logic control.

Finally, we introduce and discuss the new approach on the norm error, which measures the error at each time instant and depending on the norm the control function is produced; a switching function is generated to control the inverter switches. The parameters have been chosen such that best performance is achieved.

5.2 Three Level Hysteresis Model

Figure 5.1 shows the Simulink model for the three-level hysteresis approach [43]. The output waveforms are shown in Figure 5. 2. From Figure 5.1. (a) it gives us a hint of the speed of the controller to converge to the steady state which is called the

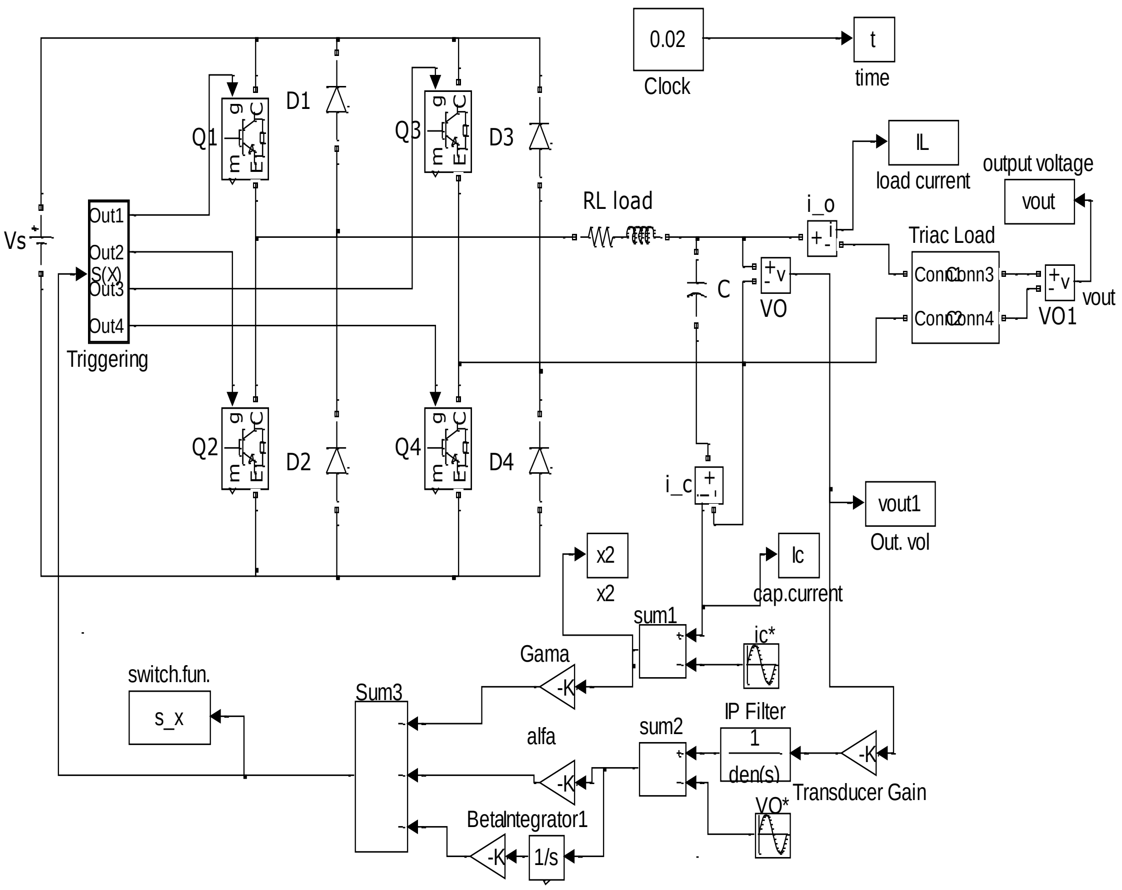

response time; here it's a bit slow.

Figure 5.1: Simulink model for three level hysterias approach [43].

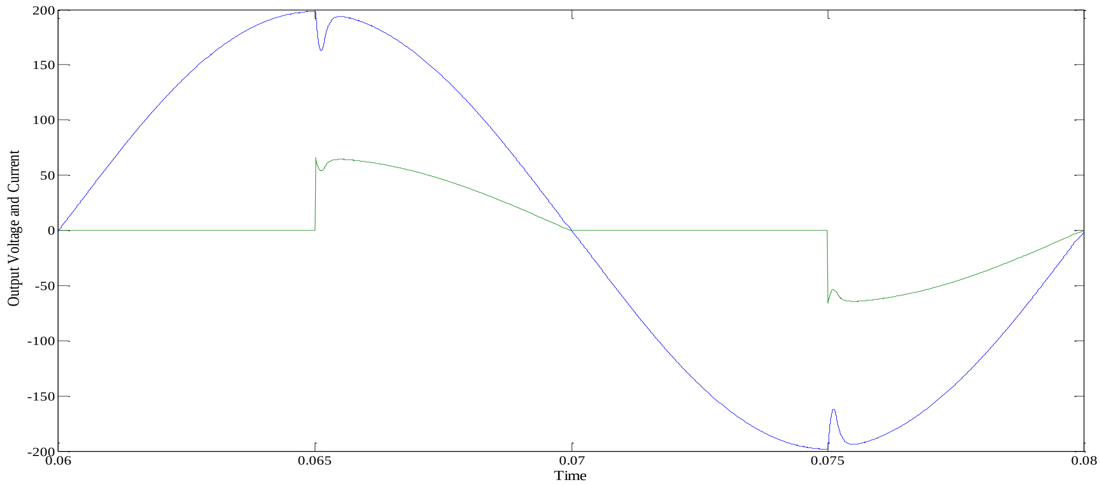
Output Voltage and Current
200
150
100
50
0
-50
-100
-150
-200
0.06
0.065
0.07
0.075
0.08
Time
(a)

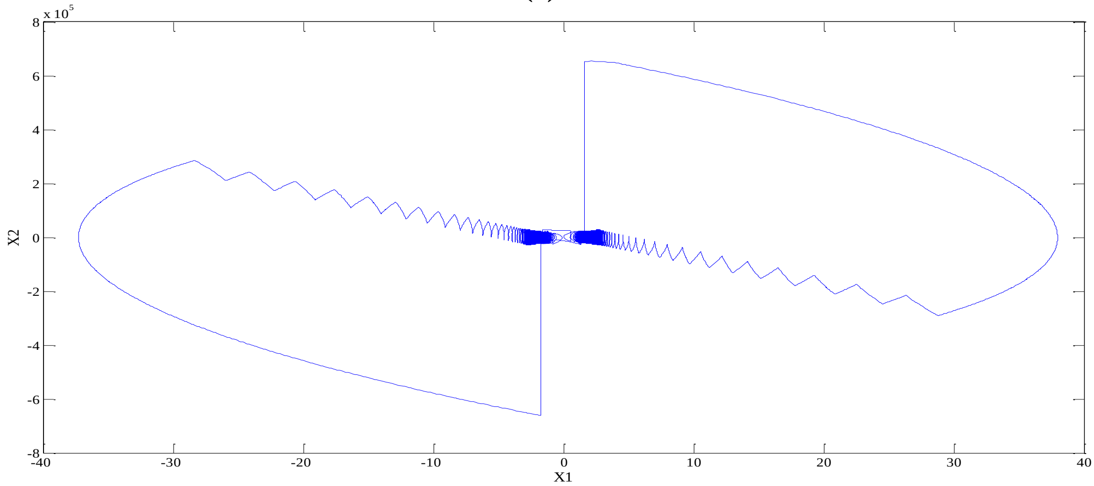
x 10^5
8
6
4
2
0
-2
-4
-6
-8
X2
-40
-30
-20
-10
0
10
20
30
40
X1
(b)

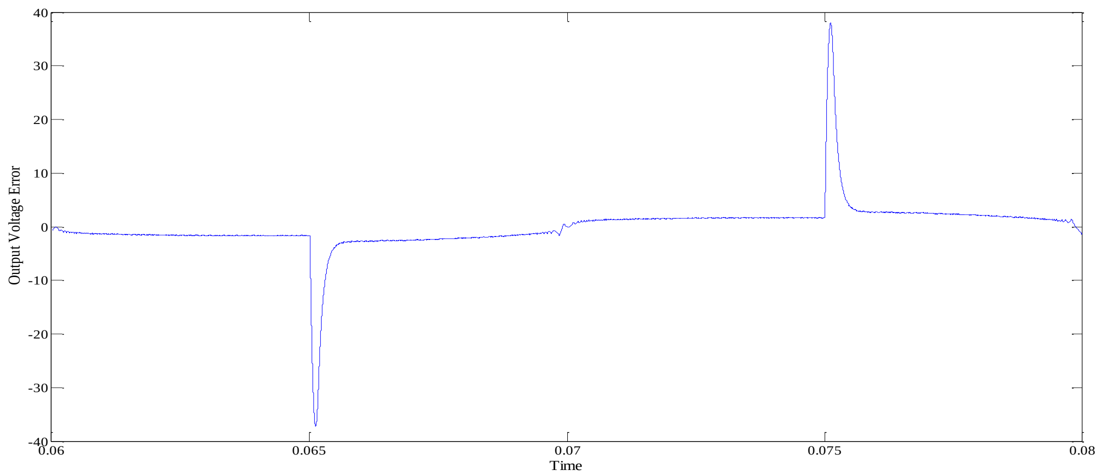
Output Voltage Error
40
30
20
10
0
-10
-20
-30
-40
0.06
0.065
0.07
0.075
0.08
Time
(c)

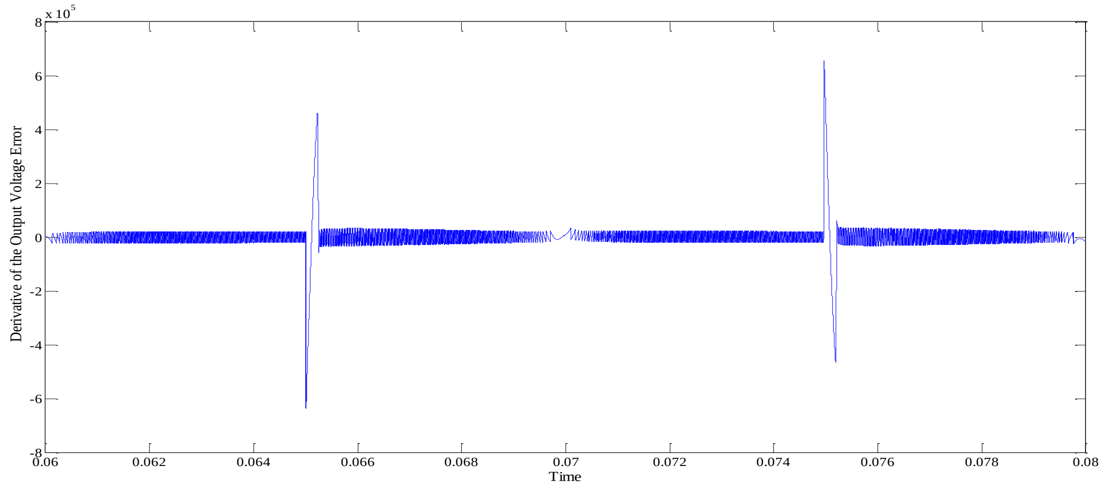

(d)

Figure 5.2: Output waveforms of three-level approach (a) output voltage. (b) phase plane portrait (c) voltage error output (d) derivative of the voltage error [43].

In Figure 5.2 (b) the chattering problem discussed in Section 3.6 is very clear. This undesired phenomenon reduces the system performance, cause heating and vibration for the controlled system. The level of the output signal in Figure 5.2 (c) shows the output voltage error, which is a good measurement to know to what degree the system can follow the reference voltage. And it's a bit large here compared with the other approaches which will follow later.

For a rectifier load applied to the output of the inverter using the three-level hysteresis, the output voltage and current are shown in Figure 5.3 with fundamental amplitude of 198 volt and 10.14A for the voltage and the current respectively.

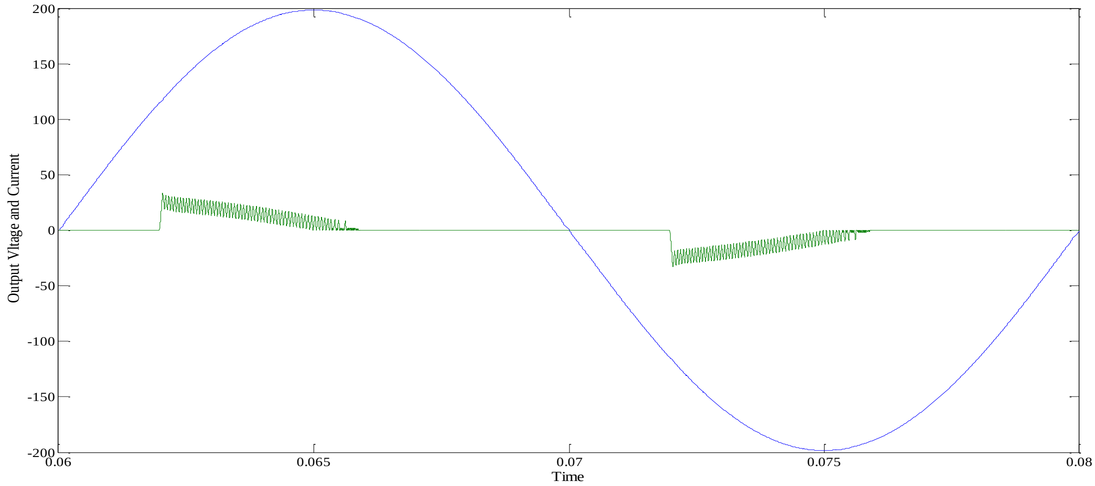

Figure 5.3: Output voltage and current waveforms for a rectifier load using three level hysteresis approach.

5.3 Rotating Sliding Line Model

Figure 5.4 shows the Matlab Simulink model for the rotating sliding-line approach [44]. The slope of the sliding line in the model below is a subsystem which contains the fuzzy logic function given by $\lambda^{FL}(t) = -0.45X_d + 0.5$ such that $X_d = |X_1| - |X_2|$ which is multiplied by another gain called K_u (in the simulation called Lambda); the resultant value of the multiplication gives the slope of the sliding line. The switching function which is given by $s = -\lambda x_1 - x_2$ aims to control the slope of the sliding line and rotates it such that the total performance is improved. The design parameters are shown in Table (5.1) which are the same as in [44], except for the hysteresis width which is taken to be the same for all the simulations mentioned before.

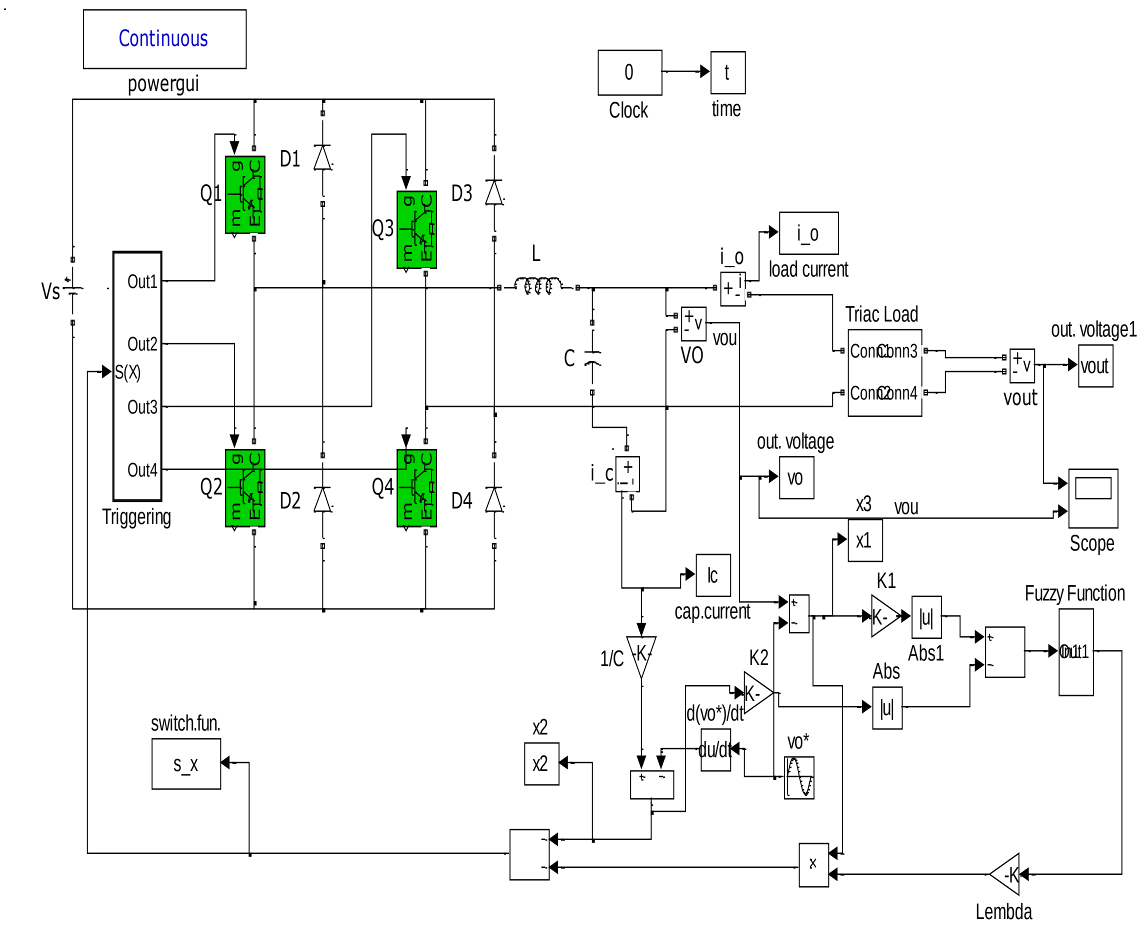

Figure 5.4: Simulink model for rotating sliding line approach [44].

The output waveforms of the voltage are shown in Figure 5.5 below.

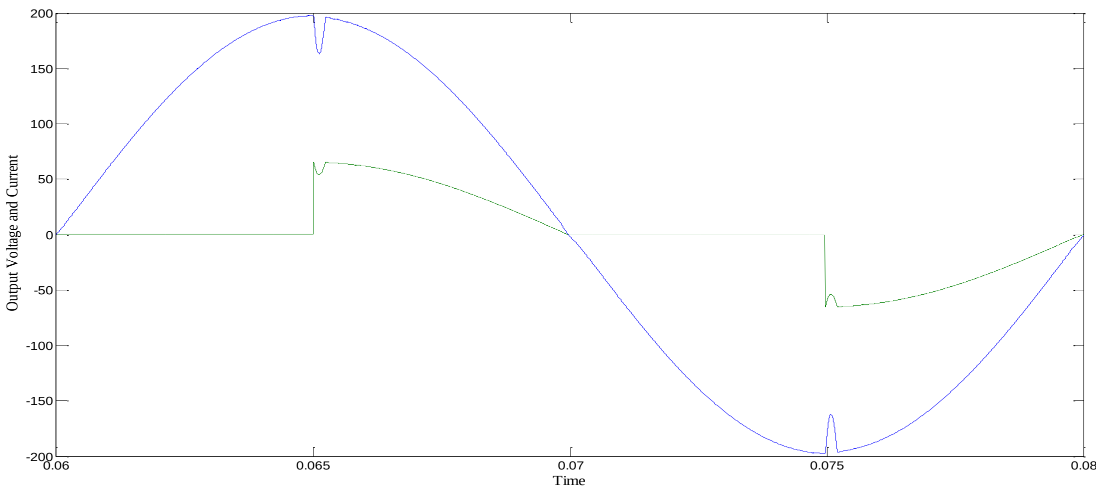

(a)

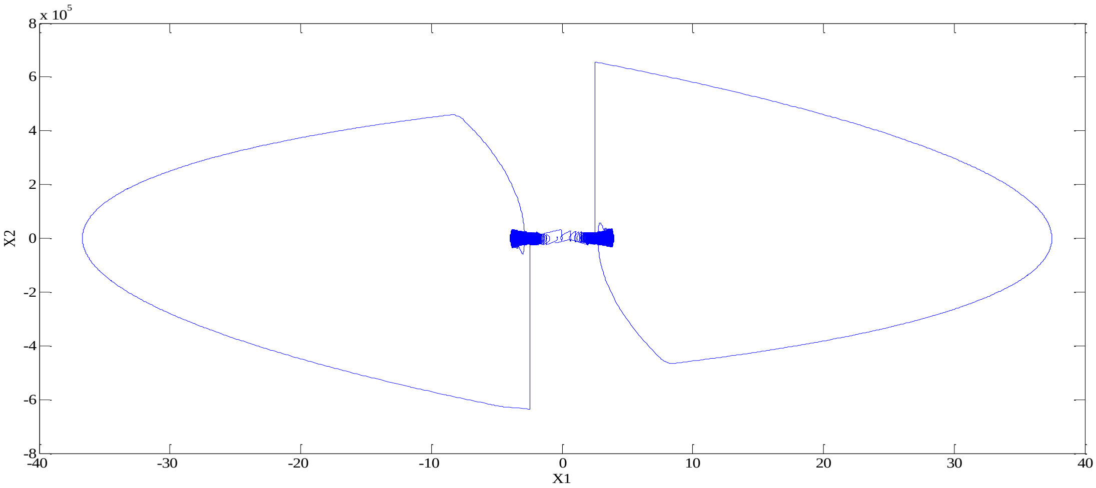

(b)

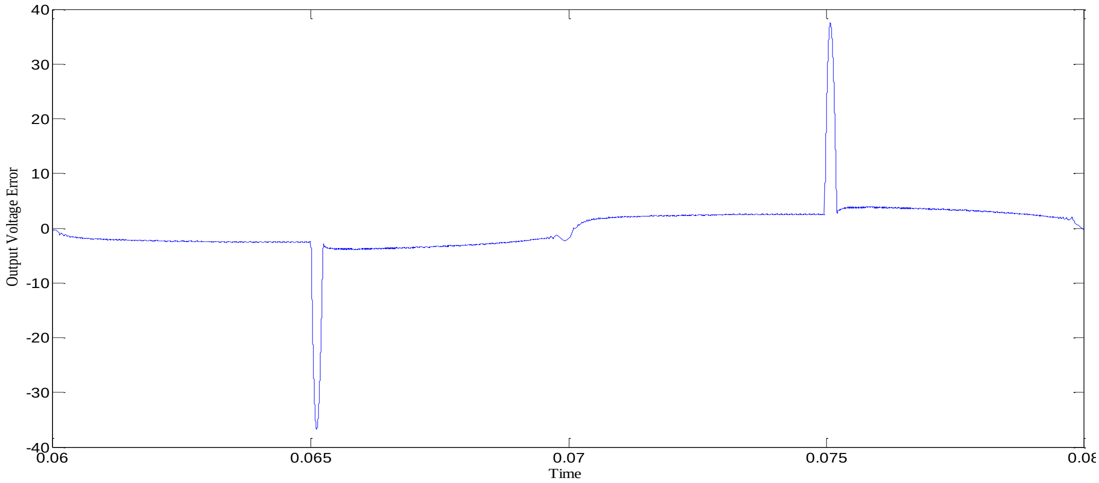

(c)

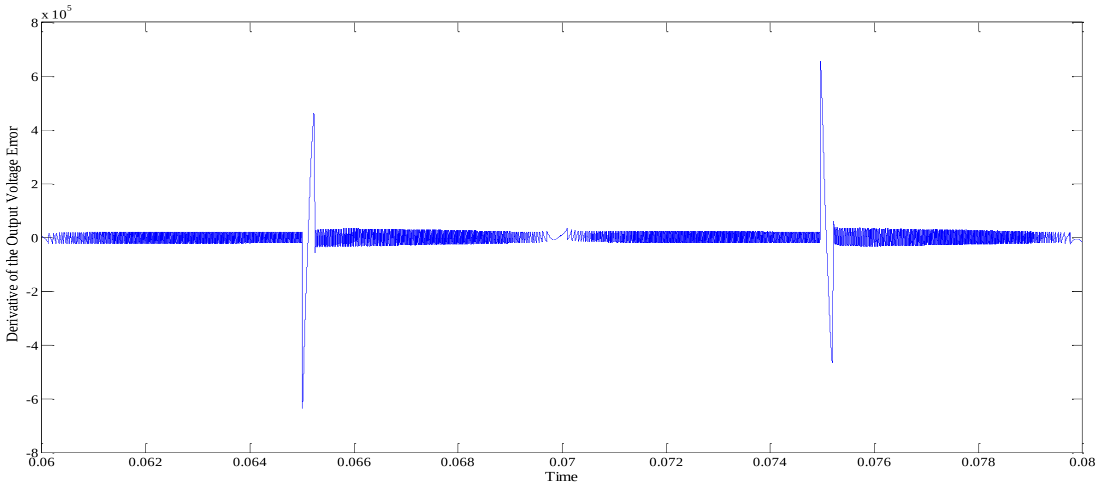

(d)

Figure 5.5: Output waveforms of RSMC (a) output voltage. (b) Phase portrait (c) voltage error output (d) derivative of the voltage error.

Notice that by rotating sliding line the chattering problem is reduced to a very small value as shown in Figure 5.5 (b), and this is one of the advantages of RSMC approach. But the steady state error is still large compared to the norm approach as shown in Figure 5.5 (c). Also here we applied a bridge rectifier load and the output voltage amplitude and current are found to be 197volt and 10.09A respectively as shown in Figure 5.6.

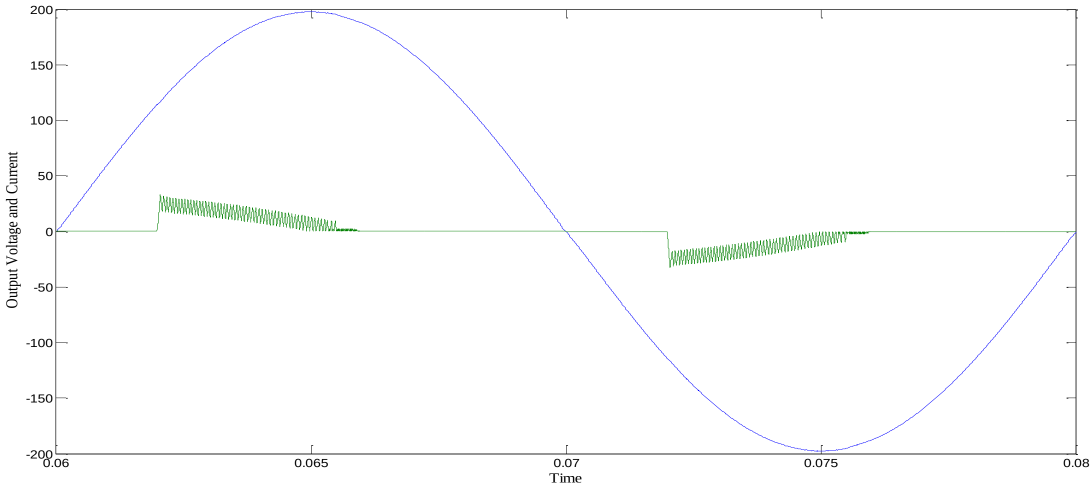

Figure 5.6: Output voltage and current waveforms for a rectifier load using rotating sliding line approach.

5.4 Norm of the Error Model

The Simulink model of the new approach is depicted in Figure 5.7. The design parameters are chosen as shown in Table 5.3 under the same conditions for the two approaches mentioned before. The output waveforms are shown in Figure 5.8.

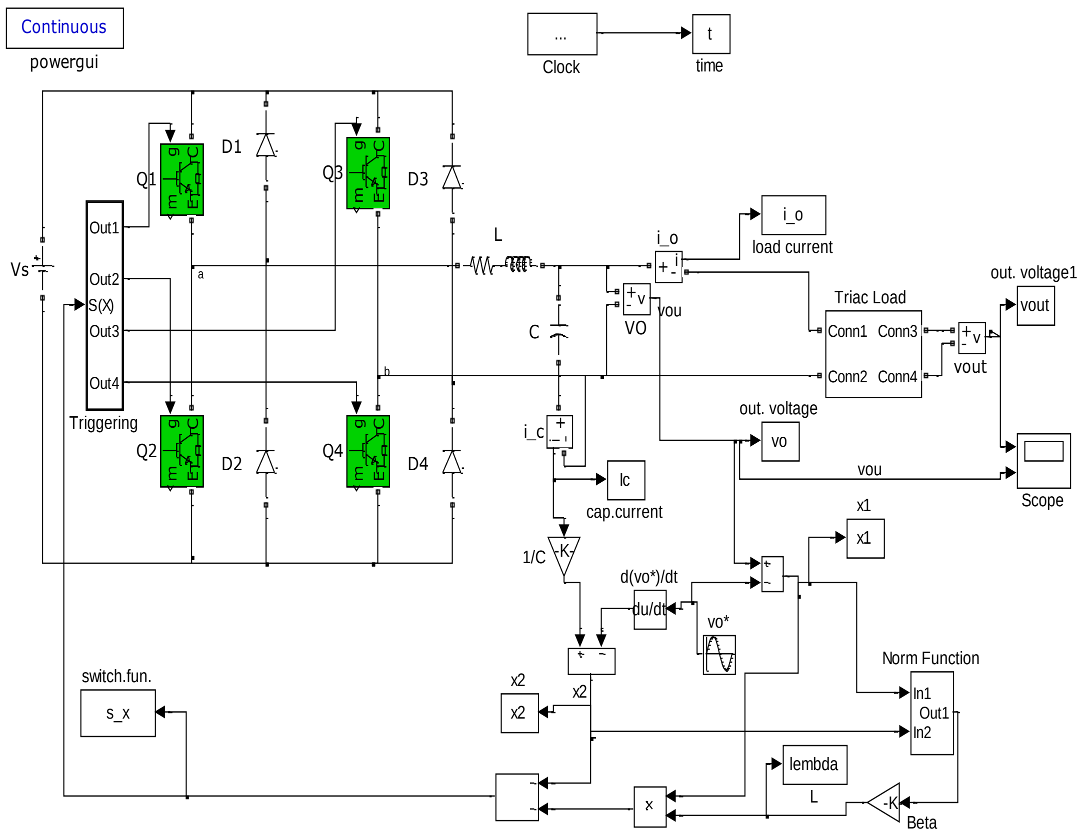

Figure 5.7: Simulink model for Norm of the error approach.

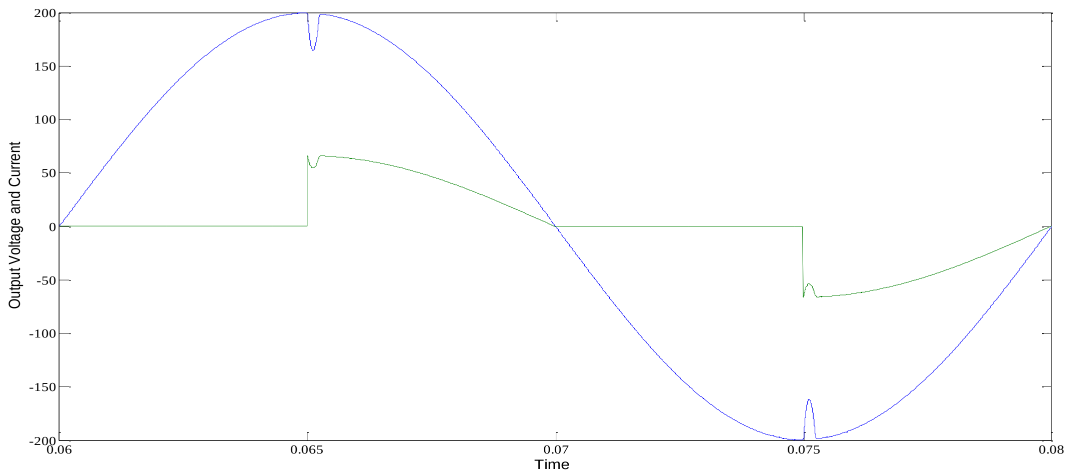

(a)

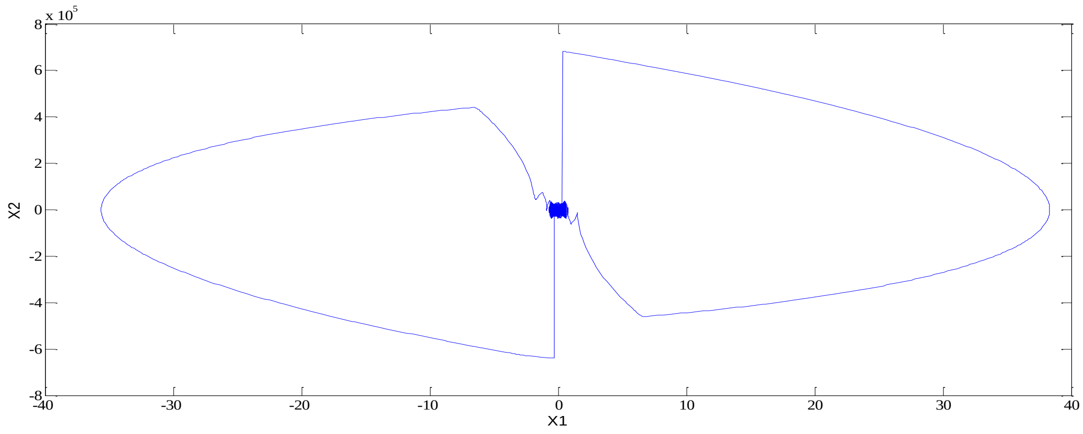

(b)

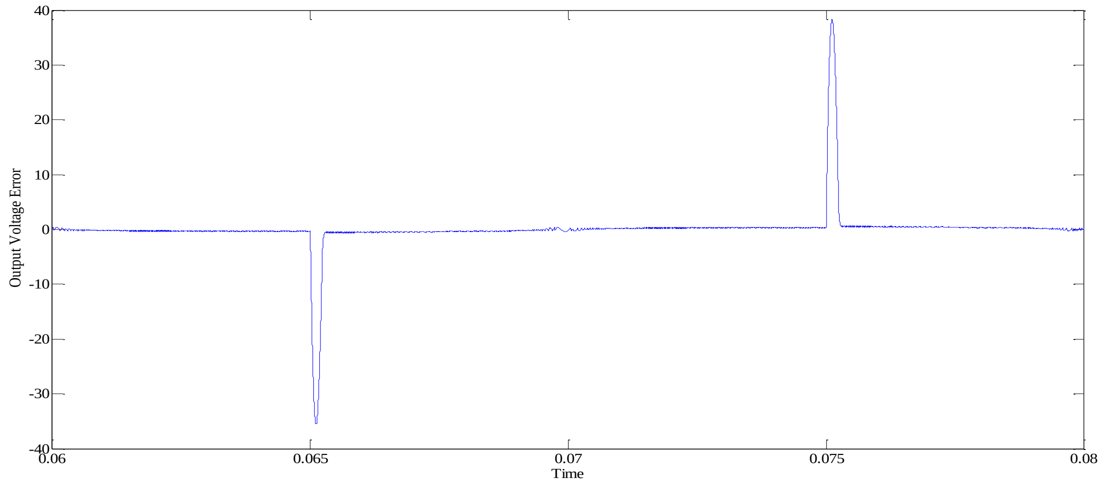

(c)

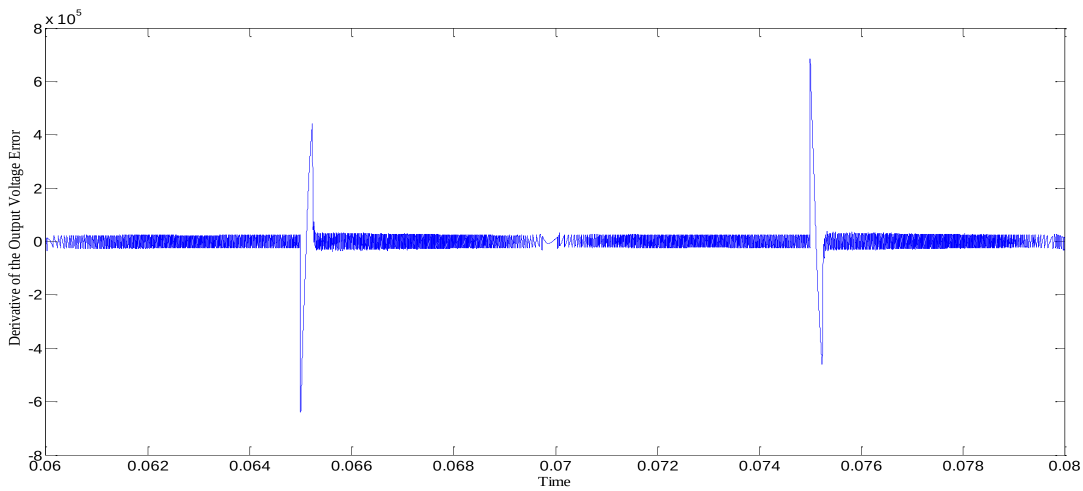

(d)

Figure 5.8: Output waveforms of the error of the norm approach (a) output voltage. (b) Phase portrait (c) voltage error output (d) derivative of the voltage error.

For full bridge rectifier load the output voltage amplitude and current are found to be 199.7V and 10.21A respectively as shown in Figure 5.9.

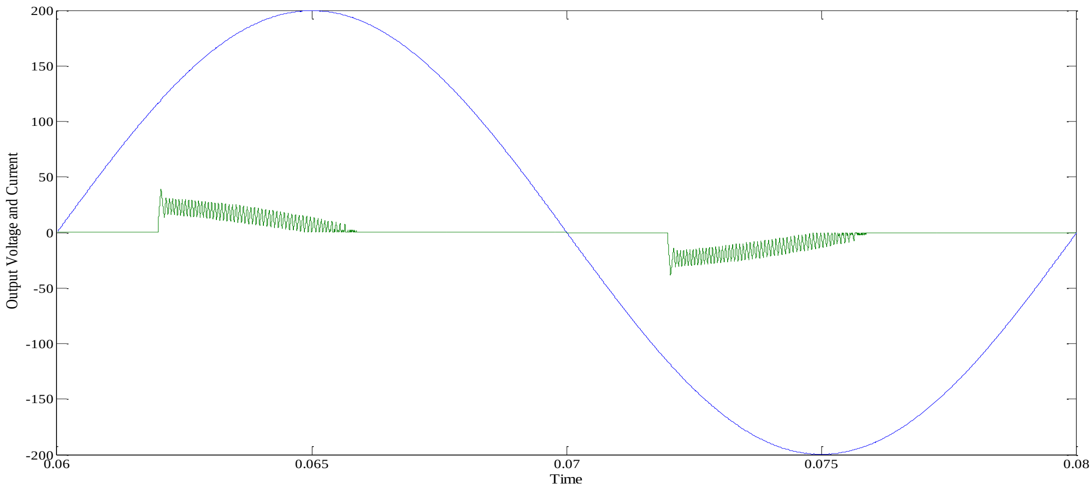

Figure 5.9: Output voltage and current waveforms for a rectifier load using norm of the error approach.

5.5 Comparison of Results

The impact of response speed and the convergence of the system to the steady state can be observed from Figure 5.2 (a), Figure 5.5 (a) and Figure 5.8 (a) for the three level hysteresis, rotating sliding line and the norm approach respectively. Figure 5.8 (a) shows the benefit of using the new approach in having very fast speed of convergence. The output voltage follows its reference very fast (tries to keep its sinusoidal waveform) regardless of the disturbances occurring on the load. This is also reflected directly to the amplitude of the output voltage, which is closer to the reference using the norm approach and compared with the other approaches.

From the previous figures it’s obvious that the chattering problem is a bit large for the three-level hysteresis approach, and it’s reduced to a lower level (the zigzag width is reduced) by making use of the rotating sliding line approach. The chattering problem is almost eliminated using the norm approach which is established analytically from the system parameters and which is achieving the system requirement. Notice that the amount of chattering can be reduced by reducing the value of the hysteresis width (h).

Notice that for the error norm approach when the states become close to the equilibrium point the slope of the sliding line decreases rapidly till it reaches the point x_{12} described in the theory before and shown in Figure 4.3. This is the same point shown in the simulation of the new approach in Figure 5.10, which shows a snapshot for the sliding line, equilibrium point and a part of the reaching mode.

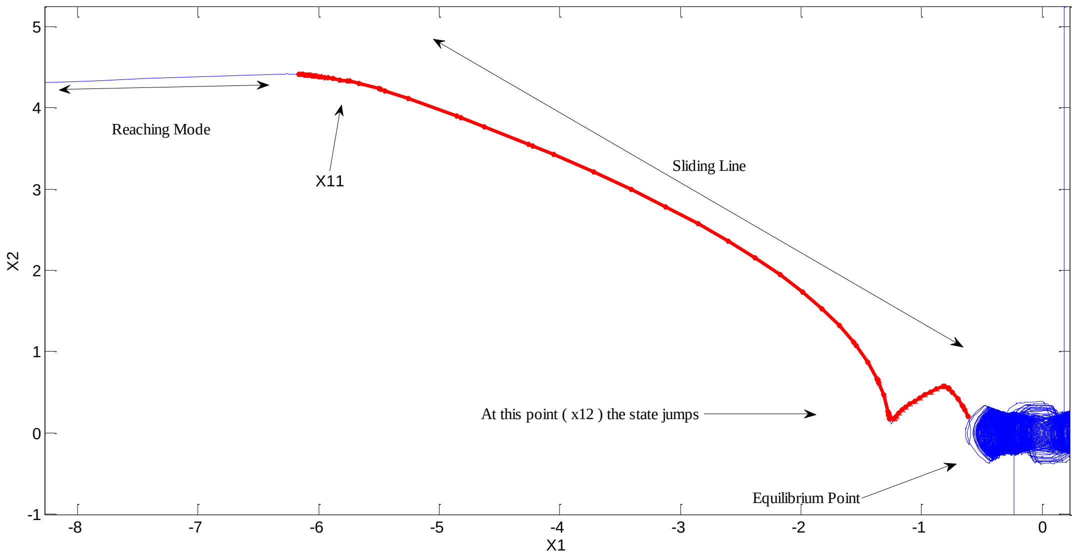

Figure 5.10: Snapshot for the sliding line, shows the "jump" occurred on it.

This is because of the nature of the algorithm used here aims to have a large slope when the trajectory hits the sliding line and starts to slide on it. The value of the slope is given by $\lambda_2 = e_2\beta$. After that when the state reaches the point x_{12} the slope of the sliding line is decreased to $\lambda_1 = e_1\beta$. When the states are very close to the equilibrium point it jumps to a new lower value of the slope which reduces the steady state error.

Tables (5.1), (5.2) and (5.3) show the system parameters for the three-level hysteresis, rotating sliding line, and the new approach respectively. All the systems are under the same conditions. Notice that the names of the parameters may vary, but the definitions are still valid.

Table 5.1: System parameters for three-level hysteresis approach [43].

Parameter	The value
V_m	200 volt
V_s	300 volt
L	250 μH
C	100 μF
Hysteresis width (h)	30,000
λ	10,000

Table 5.2: System parameters for rotating sliding line approach [44].

Parameter	Value
V_m	200 volt
V_s	300 volt
L	250 μH
C	100 μF
Hysteresis width (h)	30,000
λ	10,000
k_1	2×10^{-3}
k_2	2.4×10^{-5}

Table 5.3: System parameters for the norm approach.

Parameter	Error Norm Approach
V_m	200 volt
V_s	300 volt
L	250 μH
C	100 μF
Hysteresis width (h)	30,000
e_1 and e_2	0 and 40 resp.
λ_1 and λ_2	8 and 16 resp.
γ	1×10^{-36}
β	1×10^{4}

Figure 5.11 show a zoom shot for the amplitude of the norm approach compared to the three-level hysteresis and rotating sliding line methods. The amplitude of the output voltage for the norm approach is larger which means that the steady state error is lower. From the same figure it's easy to notice that the speed of convergence to the reference is faster for the norm approach.

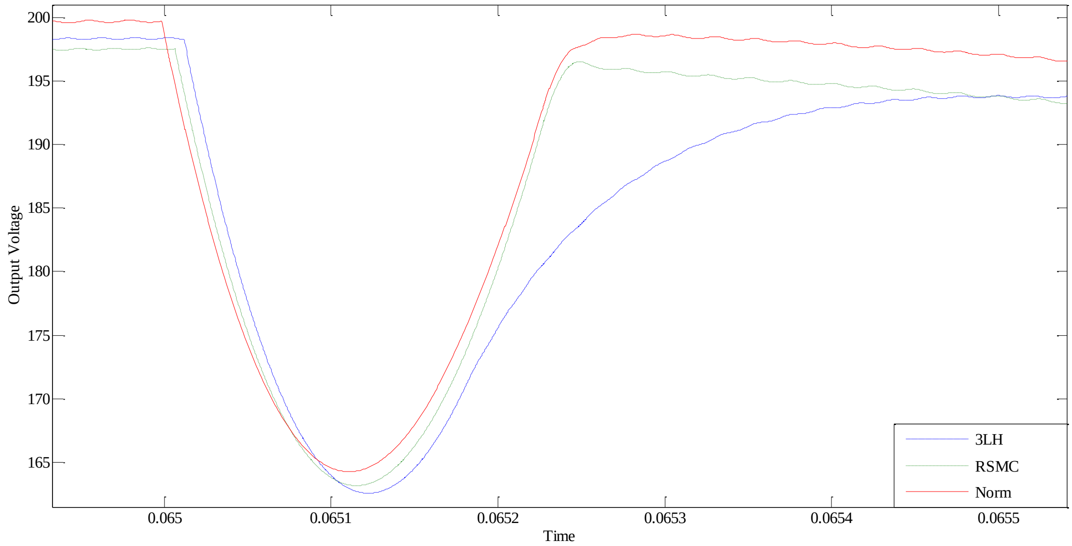

Figure 5.11: Zoom shot for the output voltages of all the approaches compared to each other.

The slope of the sliding line of the new approach is higher than those of the other approaches. This is because of the nature of the algorithm used in the norm approach which increases the slope when the trajectory hits the sliding line.

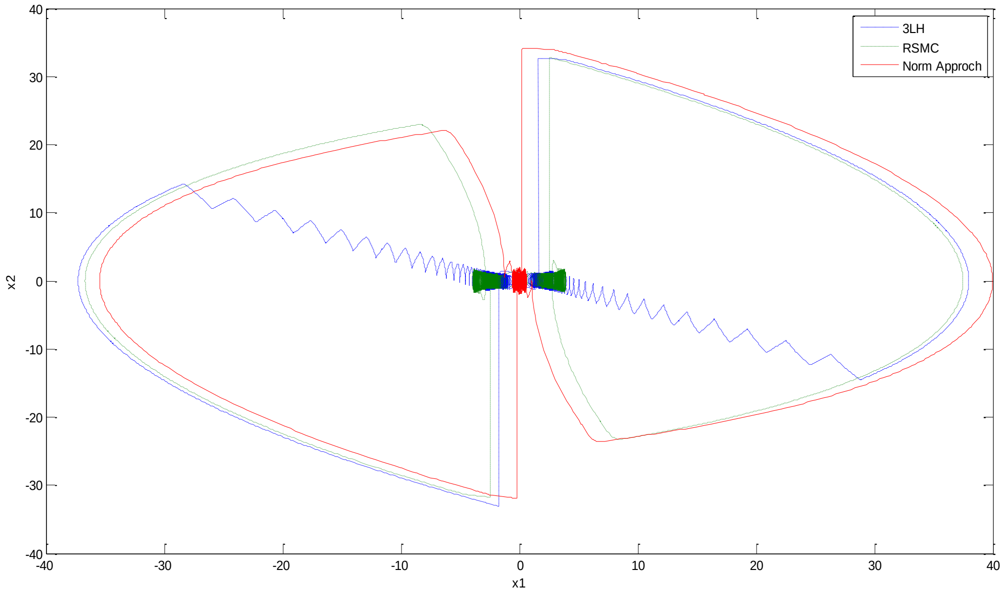

Figure 5.12: State trajectory for all the approaches.

The performance of the new approach shows a satisfactory level compared to the other approaches for both rectifier and triac loads. Table (5.4) summarizes the previous discussions.

5.6 Absolute of the Voltage Error

From equation (4.15) and its corresponding Figure 4.4 it's clear that we have to choose very small value of γ and large value of β. It's also possible to choose γ to be zero; this means that we are using the absolute value of the voltage error to determine the slope of the sliding line. Such a function is capable of reducing the THD and the error RMS value is reduced further more. Using the absolute value of the voltage error the number of parameters to be designed is reduced to be only one instead of two, which is much better and easier to work with.

The absolute of the voltage error is simulated under the same condition of the norm approach, with absolute function instead of the norm function and the results are summarized in the Table 5.4.

Table 5.4: Comparison of results of all the approaches for triac load.

Performance parameter	3LH	RSMC	Norm	Absolute
THD (%)	2.89	2.65	2.89	2.81
Error RMS	4.90	4.96	4.22	4.08
Fundamental Amplitude(volt)	196.02	195.28	198.36	198.5
2^{nd} harmonic	0.03	0.08	0.58	0
3^{rd} harmonic	1.06	0.5	1.15	1.13
4^{th} harmonic	0	0.04	0.06	0
5^{th} harmonic	1.63	1.4	1.19	1.14

Table 5.5: Comparison result of all the approaches for bridge rectifier load.

Performance parameter	3LH	RSMC	Norm	Absolute
THD (%)	0.30	0.44	0.179	0.148
Error RMS	1.43	2.18	0.22	0.219
Fundamental Amplitude(volt)	198.04	197.04	199.73	199.73
2^{nd} harmonic	0.02	0.03	0	0
3^{rd} harmonic	0.42	0.64	0.02	0.02
4^{th} harmonic	0.02	0.02	0	0
5^{th} harmonic	0.21	0.36	0	0

Notice that the total harmonic distortion is calculated for the first 400 harmonics.

Chapter 6

CONCLUSIONS AND FUTURE WORK

6.1 Conclusion

A new approach of sliding mode control is introduced which is based on the time varying slope of the sliding line applied to the system. This slope is derived from the values of the norm of the error which is computed from both the voltage error x_1 and its rate of change x_2 scaled by γ. The resultant value of the norm is applied to a saturation function which determines the value of the slope. For small values of the norm, which means that the error is small, the value of the slope (i.e. the output of the saturation function) is small, and when the value of the norm is increased the value of the slope is increased. The output norm value is multiplied by constant β. Finally the result of the multiplication is a time varying slope of the sliding mode control.

The behavior of the norm function is useful for reducing the sliding time. This means that the response time is decreased. Simulation results shows the benefit of using such a function which noticeably improve the response time, increase the amplitude of the fundamental voltage and reduce the RMS value of the voltage error.

6.2 Future Work

The equation which clearly represents the state error in terms of the system parameters helps understand the system better and design the sliding mode controller more efficiently. While in this thesis we use a linear function to accelerate the sliding mode in reaching the origin, it’s possible to use other functions which may reduce the time to reach to origin, as future work.

It’s also possible to apply the exponential reaching function to the system, which will increase the reaching speed and reduce the sliding time which will improve the efficiency of the UPS inverter system.

REFERENCES

[1] B. M. Wilamowski, J. D. Irwin, *The Industrial Electronics Handbook – Power Electronic and Motor Drives,*2nd ed., CRC Press: Taylor & Francis, 2011.

[2] B. K. Bose, *Modern Power Electronics and AC Drives*, Prentice Hall, Upper Saddle River, 2002.

[3] Liu, C., Wu, B., Zargari, N., & Xu, D., "A novel nine-switch PWM rectifier inverter topology for three-phase UPS applications*," IEEE Trans. In Power Electronics and Applications*, pp. 1-10, Sep. 2007.

[4] Ahn, Hyo-Sung, YangQuan Chen, and Kevin L. Moore. "Iterative learning control: Brief survey and categorization," *IEEE Trans. on Systems, Man, and Cybernetics, Part C: Applications and Reviews*, vol. 37 no.6, pp. 1099-1121, 2007.

[5] O. Markusson, "Model and system inversion with applications in nonlinear system identification and control," *PHD dissertation, Kungliga Tekniska Hogskolan, Sweden*, 2002.

[6] P. R. Ouyang, B. A. Petz, F. F. Xi. "Iterative learning control with switching gain feedback for nonlinear systems," *Journal of Computational and Nonlinear Dynamics, ASME*, vol. 6, Jan. 2011.

[7] K. Watanabe, E. Nobuyama, and A. Kojima. "Recent advances in control of time delay systems-a tutorial review." *Proceedings of the 35th IEEE Decision and Control*, vol. 2, 1996.

[8] D. Heng, R. Oruganti, and D. Srinivasan, "High-performance control of a UPS inverter through iterative learning based on zero-phase filtering," *IEEE conf. of Industrial Electronics Society,* vol. 2, 2004.

[9] D. Heng, R. Oruganti, and D. Srinivasan. "Analysis and design of iterative learning control strategies for UPS inverters," *IEEE Trans. on Industrial Electronics*, vol. 54, no.3, pp. 1739-1751, 2007.

[10] Wang, Youqing, Furong Gao, and Francis J. Doyle. "Survey on iterative learning control, repetitive control, and run-to-run control," *IEEE Journal of Process Control*, vol. 9, no. 10, pp. 1589-1600, 2009.

[11] http://www.wikipedia.org/wiki

[12] T. Inoue, S. Iwai, M. Nakano, "High accuracy control of a proton synchrotron magnet power supply," *IEEE Proc of 8th IFAC World Congress,* Part 3, pp.3137-3142, 1981.

[13] T. Inoue, M. Nakano, S. Iwai, "High accuracy control of servomechanism for repeated contouring," *Proceedings of the 10th Annual Symposium on Incremental Motion Control Systems and Devices,* pp. 258–292, 1981.

[14] T. Inoue, “Practical repetitive control system design." *in Proc. 29th Conf. Decision and control*, pp.1673-1671, 1990.

[15] G. F. Ledwich, and A. Bolton, "Repetitive and periodic controller design,” *IEEE Proceedings of Control Theory and Applications,* vol. 140, no. 1, 1993.

[16] F. R. Shaw and K. Srinivasan, “Discrete-time repetitive control system design using the regeneration spectrum“’ *ASME Trans. J. Dyn. Sys., Meas., and control,* vol. 115, pp.228-237, 1993.

[17] G. Hillerstrom and J.Sternby, “Application of repetitive control to a peristaltic pump,*” ASME Tms. J. Dyn. Sys., Meas., and Contr.,* vol. 116, no.4, pp.786-789,1994.

[18] N. Sadegh, , “Synthesis of a stable discrete-time repetitive controller of MIMO system,” *ASME Trans. J. Dyn. Sys., Meas., and contr.,* vol. 117, no.1, pp.92-97, 1995.

[19] Chen, Min, et al. "Design and Analysis of High Performance Control Strategy for UPS with Repetitive Control." *IEEE Telecommunications Energy Conference, 2006. INTELEC'06. 28th Annual International*,2006.

[20] Li, Min, et al. "Comparison of two repetitive control strategies of UPS inverter on saber." *IEEE 6th International Forum on Strategic Technology (IFOST),* vol. 1, 2011.

[21] Kai, Zhang, Kang Yong, Xiong Jian, Zhang Hui, and Chen Jian, "Study on an inverter with pole assignment and repetitive control for UPS applications," *IEEE conf. in Power Electronics and Motion Control,* vol. 2, pp. 650-653, 2000.

[22] V. Kučer, "Deadbeat control, pole placement, and LQ regulation," *Kybernetika,* vol. 35, no. 6, pp. 681-692, 1999

[23] J. Hetthéssy, A. Barta, R. Bars, *Dead beat controller design*, November, 2004.

[24] K. Moudgaly, *Digital Control*. John Wiley & Sons, Ltd, 2007.

[25] K. Gokhale and R. Hof, "Deadbeat microprocessor control of PWM inverter for sinusoidal output waveform synthesis," *IEEE Proc. in Power Electronics Specialist Conference,* pp. 28-36, 1985.

[26] A. Kawamura, R. Chuarayarati and T. Haneyoshi, "Deadbeat control of PWM inverter with modified pulse patterns for uninterruptible power supply," *IEEE Trans. in Ind. Electron.* vol. 35, no.2, pp. 295-300, 1988.

[27] C. Hua, “Two-level switching pattern deadbeat DSP controlled PWM inverter,” *IEEE Trans. Power Electro,* vol. 10, no. 3, pp. 310-317, 1995.

[28] O. Kukrer, and H. Komurcugil, “Deadbeat control method for single phase UPS inverters with compensation of computation delay,” IEEE *Proc. Inst. Elect. Eng. – Elect. Power Appl.,* vol. 146, pp. 123-128, January1999.

[29] Wang, Meng, Fangzheng Li, Yadong Liu, Lipei Huang, and M. Sakane. "Distributed parallel operation of modified deadbeat controlled UPS inverters." *IEEE Conf. in Power Electronics Specialists Conference,* pp. 1727-1732, 2007.

[30] V. Utkin and K.-K.D. Young, “Methods for constructing discontinuity planes in multidimensional structure variable systems,” *Aut. Remote Contr.,* vol. 39, no. 10, pt. 1, pp. 1466-1470, 1978.

[31] Slotine, E. Jean-Jacques and L.Weiping., *Applied Nonlinear Control*, Englewood Cliffs, NJ: Prentice-Hall¸ 1991.

[32] Dorling, C. M., and A. S. I. Zinober. "Robust hyperplane design in multivariable variable structure control systems," *IEEE International Journal of Control*, vol. 48, no. 5, pp. 2043-2054,1988.

[33] Landau, Ioan Doré, et al. *Adaptive Control: Algorithms, Analysis and Applications*. Springer, 2011.

[34] Chen, Min, et al. "Design and Analysis of High Performance Control Strategy for UPS with Repetitive Control." *IEEE Telecommunications Energy Conference,* 2006.

[35] L. Min, "Comparison of two repetitive control strategies of UPS inverter on saber." *IEEE International Forum on Strategic Technology (IFOST),* vol. 1, 2011.

[36] A. Raymond, H. S.Zak, and P. G. Matthews, "Variable structure control of nonlinear multivariable systems: a tutorial," *Proceedings of the IEEE,* vol. 76, no. 3, pp. 212-232, 1988.

[37] Hung H. J., W. Gao, and C. J. Hung, "Variable structure control: a survey," *IEEE Trans. on Industrial Electronics,* vol. 40, no. 1, pp. 2-22, May 1993.

[38] V. I. Utkin, "Sliding mode control design principles and applications to electric drives," *IEEE Trans. on Industrial Electronics,* vol. 40, no.1, pp. 23-36, 1993.

[39] V. I. Utkin and K.-K.D. Young, "Methods for constructing discontinuity planes in multidimensional structure variable systems," *Aut. Remote Control*, vol. 39, no. 10, pt 1, pp. 1466-1470, 1978.

[40] Dorling, C. M., and A. S. I. Zinober. "Two approaches to hyperplane design in multivariable variable structure control systems," *IEEE International Journal of Control,* vol. 44.1, pp. 65-82, 1986.

[41] Dorling, C. M., and A. S. I. Zinober, "Robust hyperplane design in multivariable variable structure control systems," *IEEE International Journal of Control,* vol. 48.5, pp. 2043-2054, 1988.

[42] W. Gao, and James C. Hung. "Variable structure control of nonlinear systems: a new approach," *IEEE Trans on Industrial Electronics,* vol. 40.1, pp. 45-55, 1993.

[43] O. Kukrer, H. Komurcugil, and A. Doganalp, "A three-level hysteresis function approach to the sliding-mode control of single-phase UPS inverters," *IEEE Transactions on Industrial Electronics,* vol. 56, no. 9, pp. 3477-3486, 2009.

[44] H. Komurcugil, "Rotating-Sliding-Line-Based Sliding-Mode Control for Single-Phase UPS Inverters." *IEEE Transactions on. Industrial Electronics,* vol. 59, no. 10, pp. 3719-3726, 2012.

[45] B. Francis, W. Wonham, "The internal model principle for linearmultivariable regulators," *Appl. Math. Optim*. vol. 2, pp. 170–194, 1975.

APPENDICES

Appendix A: Solution of Equation (4.14)

$$\int \frac{(1-ax_1^2)^{1/2}}{x_1^2} = -[\frac{\sqrt{1-ax_1^2}}{x_1} + \sqrt{a}\sin^{-1}(\sqrt{a}x)] \quad \text{(A. 1)}$$

$$-\left[\frac{\sqrt{1-ax_1^2}}{x_1} + \sqrt{a}\sin^{-1}(\sqrt{a}x)\right]_{x_{11}}^{x_{12}} = \beta(t-t_1) \quad \text{(A. 2)}$$

In the above equations x_{11} is the initial value of x_1 at the sliding surface and x_{12} is the value of x_1 at time t_2, which could be found from (4. 11) at point e_2, where $e_2 = \frac{|x_{11}|}{(1-\gamma\beta^2 x_{11}^2)^{1/2}}$, and from Figure 4.2, $e_2 = \frac{\lambda_2}{\beta}$. Equating both equations and squaring both sides gives

$$\frac{x_{11}^2}{(1-\gamma\beta^2 x_{11}^2)} = \frac{\lambda_2^2}{\beta^2} \quad \text{(A. 3)}$$

From (A.3)

$$\beta^2 x_{11}^2 = \frac{\lambda_2^2}{(1+\gamma\lambda_2^2)}.$$

Again if you substitute this value in (A. 3) the equation will be

$$(1-\gamma\beta^2 x_{11}^2) = \frac{\beta^2 x_{11}^2}{\lambda_2^2} = \frac{1}{(1+\gamma\lambda_2^2)} \quad \text{(A. 4)}$$

Notice that from (A. 4), the denominator will be always positive. This means that there is always solution for the system given by (4.13).

From (A. 4) and (4. 11)

$$|x_{11}| = \frac{\lambda_2}{\beta(1+\gamma\lambda_2^2)^{1/2}} \quad \text{(A. 5)}$$

Following the same steps x_{12} is given by

$$|x_{12}| = \frac{\lambda_1}{\beta(1+\gamma\lambda_1^{\;2})^{1/2}} \tag{A. 6}$$

The above two equations are useful in the next step. Returning back to solve (A.2), after substituting the limits of the integral, (A.2) gives

$$-\frac{\sqrt{1-ax_{12}^{\;2}}}{x_{12}} - \sqrt{a}\sin^{-1}(\sqrt{a}x_{12}) + \frac{\sqrt{1-ax_{11}^{\;2}}}{x_{11}} + \sqrt{a}\sin^{-1}(\sqrt{a}x_{11}) = \beta(t_2 - t_1) \tag{A. 7}$$

Firstly the term $1-ax_{12}^{\;2}$ is given by

$$\frac{(1-\gamma\beta^2)\lambda_1^{\;2}}{\beta^2(1+\gamma\lambda_1^{\;2})^{1/2}} = \frac{1}{1+\gamma\lambda_1^{\;2}} \tag{A. 8}$$

Substituting x_{12} we find

$$\frac{\sqrt{1-ax_{12}^{\;2}}}{x_{12}} = \frac{\beta}{\lambda_1}\operatorname{sgn}(x_{12})$$

By following the same steps we can find that

$$\frac{\sqrt{1-ax_{11}^{\;2}}}{x_{11}} = \frac{\beta}{\lambda_2}\operatorname{sgn}(x_{11}).$$

In (A. 7) the two terms are simplified. Next the aim is to simplify the second two terms

$$\sqrt{a}\left[\sin^{-1}(\sqrt{a}x_{11}) - \sin^{-1}(\sqrt{a}x_{12})\right] \tag{A. 9}$$

Which could be simplified by assuming that $\theta_1 = \sin^{-1}(\sqrt{a}x_{11})$, $\theta_2 = \sin^{-1}(\sqrt{a}x_{12})$, $\alpha_1 = \sqrt{a}x_{11}$ and $\alpha_2 = \sqrt{a}x_{12}$. Then $\sin(\theta_1) = \alpha_1$, $\sin(\theta_2) = \alpha_2$, $\cos(\theta_1) = \sqrt{1-\alpha_1^{\;2}}$ and $\cos(\theta_2) = \sqrt{1-\alpha_2^{\;2}}$.

Using the trigonometric identity

$$\sin(\theta_1 - \theta_2) = \sin(\theta_1)\cos(\theta_2) - \sin(\theta_2)\cos(\theta_1) \tag{A. 10}$$

this will give

$$\sin(\theta_1 - \theta_2) = \alpha_1\sqrt{1-\alpha_2{}^2} - \alpha_2\sqrt{1-\alpha_1{}^2} \tag{A. 11}$$

Substituting (A. 10) into (A. 9) gives

$$\sqrt{a}\left\{x_{11}\sqrt{1-ax_{12}{}^2} - x_{12}\sqrt{1-ax_{11}{}^2}\right\} \tag{A. 12}$$

After substituting the value of $a = \gamma\beta^2$, x_{11} and x_{12}, and taking the $\sin^{-1}$, (A. 10) will become

$$\sin^{-1}\left\{\sqrt{\gamma}\frac{(\lambda_2 - \lambda_1)}{[(1+\gamma\lambda_1{}^2)(1+\gamma\lambda_2{}^2)]^{1/2}}\right\} \tag{A. 13}$$

Now, by substituting (A. 11) and the first two terms in (A. 7)

$$\beta(t_2 - t_2) = \frac{\beta}{\lambda_2}\operatorname{sgn}(x_{11}) - \frac{\beta}{\lambda_1}\operatorname{sgn}(x_{12})\sin^{-1}\left\{\sqrt{\gamma}\frac{(\lambda_2 - \lambda_1)}{[(1+\gamma\lambda_1{}^2)(1+\gamma\lambda_2{}^2)]^{1/2}}\right\} \tag{A. 12}$$

Appendix B: Contents of the Norm Block

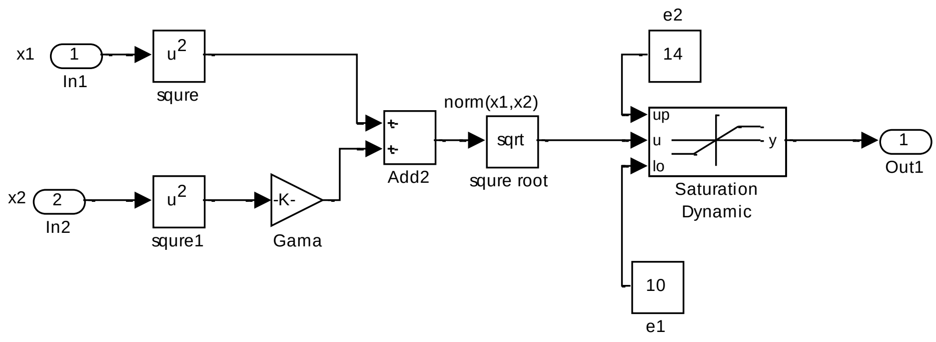

Appendix C: Contents of the Triggering Block

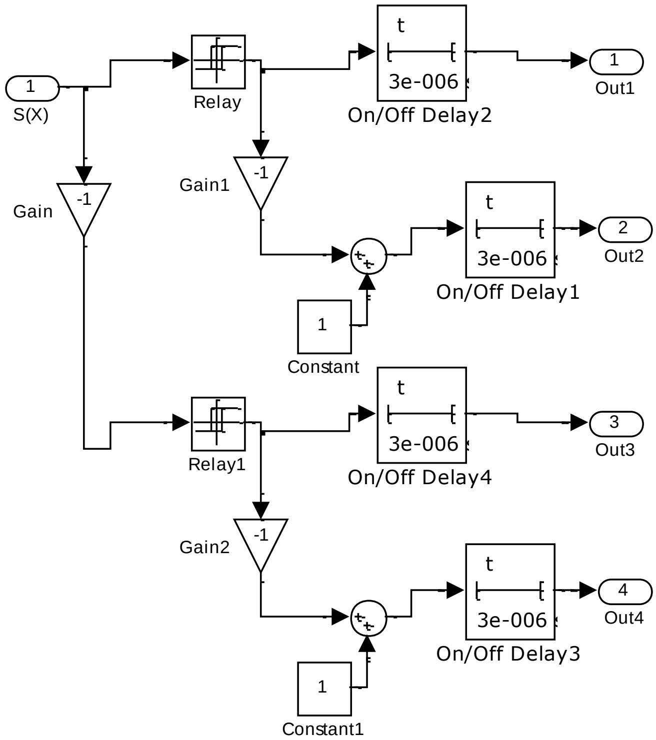

Appendix D: Matlab Code for Plotting Figure 4.4.

```
G0=0:1.e-6:0.3;
Ga=G0;
sgnx11=-1; sgnx12=-1; L1=9; L2=10;
Beta1=500;

for n=1:length(Ga)
 theta=(asind(sqrt(Ga(n))*(L2-L1)/sqrt((1+Ga(n)*L2^2)*(1+Ga(n)*L1^2))));
 time1(n)=sgnx11/L2-sgnx12/L1+theta/Beta1;
end

Beta2=600;

for n=1:length(Ga)
 theta=(asind(sqrt(Ga(n))*(L2-L1)/sqrt((1+Ga(n)*L2^2)*(1+Ga(n)*L1^2))));
 time2(n)=sgnx11/L2-sgnx12/L1+theta/Beta2;
end
Beta3=700;

for n=1:length(Ga)
 theta=(asind(sqrt(Ga(n))*(L2-L1)/sqrt((1+Ga(n)*L2^2)*(1+Ga(n)*L1^2))));
 time3(n)=sgnx11/L2-sgnx12/L1+theta/Beta3;
end
Beta4=800;

for n=1:length(Ga)
 theta=(asind(sqrt(Ga(n))*(L2-L1)/sqrt((1+Ga(n)*L2^2)*(1+Ga(n)*L1^2))));
 time4(n)=sgnx11/L2-sgnx12/L1+theta/Beta4;
end

plot(Ga,time1,Ga,time2,Ga,time3,Ga,time4)
xlabel ('Gama')
ylabel ('Time')
%%% %%% %%% %%% %%%
```